

# Peach Palm Fruit (*Bactris gasipaes*) Peel: A Source of Provitamin A Carotenoids to Develop Emulsion-Based Delivery Systems

Jader Martínez-Girón, Cinzia Cafarella, Francesca Rigano, Daniele Giuffrida, Luigi Mondello, Yolima Baena, Coralia Osorio,\* and Luis Eduardo Ordóñez-Santos



Cite This: *ACS Omega* 2024, 9, 28738–28753



Read Online

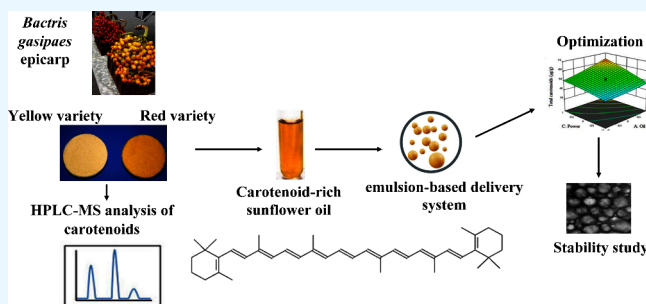
ACCESS |

Metrics & More

Article Recommendations

Supporting Information

**ABSTRACT:** The peach palm fruit (*Bactris gasipaes*) peel is a byproduct after fruit consumption. The peel flour of two varieties (yellow and red) was separately obtained by hot air drying and was subsequently milled. The proximate analysis showed that the red variety exhibited higher protein, fat, and fiber contents than the yellow one. A higher carotenoid ( $836.5 \pm 24.5 \mu\text{g/g}$ ), phenolic compounds ( $83.17 \pm 1.76 \text{ mg GAE}/100 \text{ g}$ ), and provitamin A activity ( $33.10 \pm 0.83 \mu\text{g retinol/g}$ ) were found in the cooked red variety. The carotenoid and phenolic compositions were analyzed by HPLC-PDA-MS, finding  $\beta$ -carotene and  $\gamma$ -carotene to be major compounds. The effect of thermal treatment increased the amount



of these provitamin A carotenoids and lycopene, which were detected only in the red variety. Among phenolic compounds, procyanidin dimer (isomer I), feruloyl quinic acid, and several apigenin C-hexosides were identified as major constituents of peach palm epicarp. A carotenoid-rich emulsion-based delivery system was obtained after the optimization (RSM model) of carotenoid extraction with ultraturax and sunflower oil and further development of an ultrasound-assisted emulsion. The best conditions for a stable emulsion were 73.75% water, 25% carotenoid-rich oil extract, 1.25% emulsifiers, and 480 W of ultrasonic power for 5 min. The optimized emulsion had a total carotenoid content of  $67.61 \mu\text{g/g}$ , Provitamin A activity of  $3.23 \pm 0.56 \mu\text{g RAE/g}$ , droplet size of 502.23 nm, polydispersity index of 0.170, and zeta potential of  $-32.26 \text{ mV}$ . This emulsion was chemically and physically stable for 35 days at  $30 \pm 2 \text{ }^\circ\text{C}$ , showing potential as a food additive with biofunctional properties. The strategy here developed is an economical and environmentally friendly process that allows the reuse of the byproduct of *B. gasipaes*.

## INTRODUCTION

One of the current trends of the circular economy within the framework of applying the biorefinery concept consists of giving added value to the byproducts generated after the consumption and/or transformation of fruits and vegetables.<sup>1</sup> Many of these byproducts are an important source of bioactive compounds, such as carotenoid pigments<sup>2</sup> and phenolic compounds.<sup>3</sup> *Bactris gasipaes* (Areaceae) is a tropical fruit highly consumed in the central and north parts of South America after boiling in hot water. It is called *chontaduro* or *cachipay* in Colombia, *pejibaye* in Costa Rica, and *pupunha* in Brazil. The most consumed varieties are yellow and red (Figure 1). This palm is economically relevant in the southwest of Colombia, with a production of 7793 tn/year during 2023.<sup>4</sup> The weight of the fruit varies between 20 and 100 g and is composed of the mesocarp (ca. 72%), the epicarp (ca. 16%) or peel, and the hard seed (ca. 12%).<sup>5</sup> The cooked fruit pulp is consumed as a snack accompanied by salt or honey, and the epicarp is usually discarded as residual biomass. However, the flour obtained by drying fruit epicarp showed to be a potential bioresource of bioactive compounds, such as phenolic

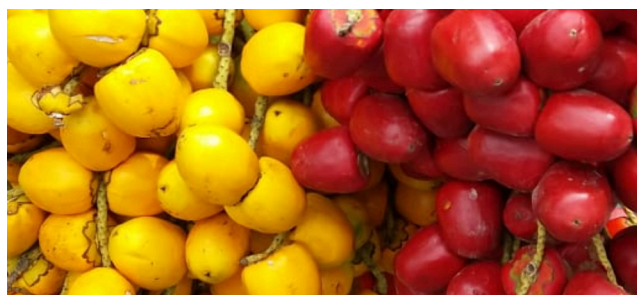


**Figure 1.** Yellow and red varieties of peach palm fruits (*Bactris gasipaes*) from Valle del Cauca, Colombia.

Received: March 31, 2024

Revised: June 8, 2024

Accepted: June 11, 2024

Published: June 18, 2024



**Table 1. Physicochemical Characterization of Peach Palm Fruit (*Bactris gasipaes*) Peel Flours Obtained by Different Drying Methods<sup>a</sup>**

parameter	YVFD	RVFD	YVHAD	RVHAD
dry matter (%)	93.89 ± 0.16 <sup>a</sup>	94.12 ± 0.55 <sup>a</sup>	89.25 ± 0.53 <sup>b</sup>	89.14 ± 0.37 <sup>b</sup>
water activity (a <sub>w</sub> )	0.35 ± 0.03 <sup>b</sup>	0.34 ± 0.02 <sup>b</sup>	0.43 ± 0.01 <sup>a</sup>	0.44 ± 0.02 <sup>a</sup>
pH	4.86 ± 0.14 <sup>c</sup>	5.09 ± 0.13 <sup>b</sup>	5.14 ± 0.10 <sup>ab</sup>	5.46 ± 0.11 <sup>a</sup>
acidity (% citric acid)	0.29 ± 0.06 <sup>a</sup>	0.23 ± 0.03 <sup>ab</sup>	0.24 ± 0.04 <sup>ab</sup>	0.19 ± 0.05 <sup>c</sup>
ash (%)	1.92 ± 0.38 <sup>ab</sup>	1.77 ± 0.64 <sup>c</sup>	2.12 ± 0.05 <sup>a</sup>	1.85 ± 0.03 <sup>bc</sup>
proteins (%)	6.14 ± 0.32 <sup>bc</sup>	7.24 ± 0.86 <sup>a</sup>	5.86 ± 0.23 <sup>c</sup>	6.87 ± 0.15 <sup>b</sup>
lipids (%)	8.39 ± 0.61 <sup>c</sup>	12.74 ± 0.47 <sup>b</sup>	9.65 ± 0.17 <sup>bc</sup>	14.21 ± 0.13 <sup>a</sup>
carbohydrates (%)	77.44 ± 0.26 <sup>a</sup>	72.37 ± 0.33 <sup>b</sup>	71.62 ± 0.16 <sup>ab</sup>	66.21 ± 0.10 <sup>c</sup>
crude fiber (%)	9.16 ± 0.39 <sup>c</sup>	13.76 ± 0.72 <sup>b</sup>	10.34 ± 0.86 <sup>bc</sup>	16.56 ± 0.42 <sup>a</sup>
color parameters				
L*	61.10 ± 3.45 <sup>b</sup>	73.06 ± 3.75 <sup>a</sup>	35.87 ± 1.74 <sup>d</sup>	46.09 ± 2.29 <sup>c</sup>
a*	1.34 ± 0.31 <sup>d</sup>	3.14 ± 0.89 <sup>c</sup>	7.38 ± 0.73 <sup>b</sup>	21.59 ± 1.25 <sup>a</sup>
b*	20.42 ± 1.18 <sup>d</sup>	27.63 ± 2.39 <sup>c</sup>	39.25 ± 1.84 <sup>b</sup>	58.12 ± 3.71 <sup>a</sup>
C <sub>ab</sub> *	20.46 ± 0.56 <sup>d</sup>	27.80 ± 1.12 <sup>c</sup>	39.94 ± 1.59 <sup>b</sup>	62.01 ± 2.85 <sup>a</sup>
h <sub>ab</sub>	86.24 ± 1.38 <sup>ab</sup>	83.51 ± 3.31 <sup>ab</sup>	79.35 ± 2.76 <sup>b</sup>	69.62 ± 3.74 <sup>c</sup>
IC*	1.07 ± 0.34 <sup>cd</sup>	1.55 ± 0.72 <sup>c</sup>	5.24 ± 0.23 <sup>b</sup>	8.06 ± 0.61 <sup>a</sup>
bioactive compounds				
total carotenoids (μg/g, DW)	43.0 ± 6.1 <sup>d</sup>	481.9 ± 25.8 <sup>b</sup>	75.0 ± 7.7 <sup>c</sup>	836.5 ± 24.5 <sup>a</sup>
vitamin A (μg RAE/g, DW)	2.30 ± 0.17 <sup>cd</sup>	20.90 ± 0.54 <sup>b</sup>	3.90 ± 0.19 <sup>c</sup>	33.10 ± 0.83 <sup>a</sup>
total phenolic content (mg GAE/100g, DW)	33.75 ± 1.28 <sup>c</sup>	91.39 ± 2.36 <sup>a</sup>	26.12 ± 1.34 <sup>d</sup>	83.17 ± 1.76 <sup>b</sup>

<sup>a</sup>YVFD: Yellow variety, freeze-dried, raw. RVFD: Red variety, freeze-dried, raw. YVHAD: Yellow variety, hot air-dried, cooked. RVHAD: Red variety, hot air-dried, cooked. RAE = Retinol activity equivalents. All data are the mean of three measurements ± SD. Different letters (a–d) in a field mean significant differences ( $p < 0.05$ ).

compounds ( $23.40 \pm 1.30$  mg gallic acid/100 g) and carotenoids ( $59.31 \pm 1.61$  mg  $\beta$ -carotene/100 g).<sup>6</sup>

There are many reports in the literature about the carotenoid content of raw and cooked *B. gasipaes* pulp; however, reports about carotenoids in the peel are scarce. Martínez-Girón and Ordóñez-Santos<sup>7</sup> studied the carotenoid composition in the *B. gasipaes* peel fruit flour (different varieties) obtained by drying at 60 °C and subsequent saponification. The main constituents were *trans*- $\beta$ -carotene, 13-*cis*- $\beta$ -carotene, 9-*cis*- $\beta$ -carotene, and  $\alpha$ -carotene, among others. The total amount of carotenoids quantified by HPLC was 195.7 μg/g of fruit (DB). Noronha Matos et al.<sup>5</sup> reported a carotenoid content of  $33.69 \pm 3.24$  mg/100g of raw peel fruit (DB) from Brazil (orange-colored peel), being higher than that reported for the pulp,  $3.18 \pm 0.46$  mg/100g fruit (DB). These authors also reported all-*E*- $\beta$ -carotene and all-*E*- $\gamma$ -carotene as the main constituents of the peach palm peel, showing the potential use of this agro-industrial waste as a high source of carotenoids. Recently, Menezes Silva et al.<sup>8</sup> reported a carotenoid amount of  $66.7 \pm 7.33$  mg  $\beta$ -carotene Eq/100 g fruit (DB) on the *B. gasipaes* (orange-colored peel) cooked peel from Brazil, extracted with ethanol and ultrasound. These authors also reported all-*E*- $\beta$ -carotene and all-*E*- $\gamma$ -carotene as the main constituents of the *B. gasipaes* peel.

Raw or cooked *Bactris gasipaes* fruit is also a source of phenolic compounds. Santos et al.<sup>9</sup> reported an average concentration of phenolic compounds of 2.11 mg GAE/g of DM in the flour obtained by freeze-drying fruits (mesocarp and epicarp). Chisté et al.<sup>10</sup> studied the carotenoid and phenolic composition of cooked orange and yellow *B. gasipaes* pulp fruits from Brazil. The main constituents were characterized by HPLC-PDA-ESI-MS as apigenin 6-C-hexoside 8-C-pentoside (schafostside) in both varieties, apigenin 6,8-di-C-hexoside (vicenin-2) in the orange variety, and apigenin 6-C-hexoside

sulfate (isovitexin sulfate) in the yellow variety, among other apigenin derivatives.

Some carotenoids are health-promoting food phytochemicals because they can be converted to retinol in the body, such as exhibiting provitamin A activity. Among them,  $\alpha$ -carotene,  $\beta$ -carotene, and  $\beta$ -cryptoxanthin are provitamin A carotenoids.<sup>11</sup> Also, they exhibited antioxidant activity that helps to boost the immune system.<sup>12</sup> However, there are few studies on their application in hydrophilic matrices due to their fat-soluble nature, making it necessary to use technologies such as emulsification to incorporate these bioactive compounds into different foods. The emulsion-based delivery system for carotenoids consists of two immiscible liquids, in which one liquid (oil) is dispersed as droplets in the other phase (aqueous) and stabilized by the addition of emulsifiers.<sup>13</sup> These oil-in-water (O/W) emulsions are widely used as a delivery system and also to improve the carotenoid physicochemical stability and bioaccessibility.<sup>14,15</sup>

One of the current trends is the use of environmentally friendly techniques for bioactive compound extraction from food waste or byproducts.<sup>16</sup> Among the emerging technologies, ultrasound-assisted emulsification is based on using acoustic waves, generating a cavitation effect, causing a decrease in droplet size, and allowing the homogenization of the components to stabilize the emulsion.<sup>17,18</sup> This process is considered a low-energy-consumption technology due to the short time used in homogenization. Several variables are involved in the emulsification process; thus, an experimental strategy is needed to optimize the process. For this purpose, tools such as the response surface methodology (RSM) are helpful because they lead to statistically robust results, including axial and central points, which allow significant evidence of the effect and interactions of the factors on the response variables of interest, using 3D contour diagrams.<sup>19</sup> Thus, this work aimed to physicochemically characterize the

**Table 2. Carotenoid Composition of Peach Palm Fruit (*Bactris gasipaes*) Peel Flours Obtained by Different Drying Methods<sup>a</sup>**

no.	RT (min)	compound	YVFD	RVFD	YVHAD	RVHAD
1	48.1	13- <i>cis</i> - $\beta$ -carotene	2.5 $\pm$ 0.8 <sup>cd</sup>	33.8 $\pm$ 2.1 <sup>b</sup>	4.2 $\pm$ 0.7 <sup>c</sup>	63.8 $\pm$ 2.8 <sup>a</sup>
2	51.7	$\alpha$ -carotene	1.5 $\pm$ 0.4 <sup>cd</sup>	10.5 $\pm$ 1.9 <sup>b</sup>	2.8 $\pm$ 0.8 <sup>c</sup>	36.8 $\pm$ 1.9 <sup>a</sup>
3	57.9	$\beta$ -carotene	26.7 $\pm$ 1.6 <sup>d</sup>	197.3 $\pm$ 4.7 <sup>b</sup>	43.6 $\pm$ 1.6 <sup>c</sup>	285.7 $\pm$ 6.8 <sup>a</sup>
4	60.8	9- <i>cis</i> - $\beta$ -carotene	6.2 $\pm$ 0.9 <sup>d</sup>	22.5 $\pm$ 2.1 <sup>b</sup>	10.8 $\pm$ 1.2 <sup>c</sup>	62.6 $\pm$ 2.4 <sup>a</sup>
5	72.2	$\delta$ -carotene	1.7 $\pm$ 0.8 <sup>cd</sup>	39.3 $\pm$ 1.8 <sup>b</sup>	2.6 $\pm$ 1.2 <sup>c</sup>	62.9 $\pm$ 1.3 <sup>a</sup>
6	82.8	<i>Z</i> - $\gamma$ -carotene	2.5 $\pm$ 0.8 <sup>cd</sup>	35.5 $\pm$ 1.2 <sup>b</sup>	4.3 $\pm$ 0.8 <sup>c</sup>	77.3 $\pm$ 1.7 <sup>a</sup>
7	83.8	$\gamma$ -carotene	1.9 $\pm$ 0.8 <sup>d</sup>	98.1 $\pm$ 2.1 <sup>b</sup>	5.1 $\pm$ 0.8 <sup>c</sup>	188.2 $\pm$ 4.7 <sup>a</sup>
8	107.7	lycopene	n.d	44.9 $\pm$ 3.8 <sup>b</sup>	1.6 $\pm$ 0.6 <sup>c</sup>	59.2 $\pm$ 2.9 <sup>a</sup>

<sup>a</sup>RT = retention time in C<sub>30</sub> HPLC column. YVFD: Yellow variety, freeze-dried, raw. RVFD: Red variety, freeze-dried, raw. YVHAD: Yellow variety, hot air-dried, cooked. RVHAD: Red variety, hot air-dried, cooked. All data are the mean of three measurements  $\pm$  SD and expressed in  $\mu$ g/g, dw. Different letters in a file mean significant differences ( $p < 0.05$ ). n.d = not determined.

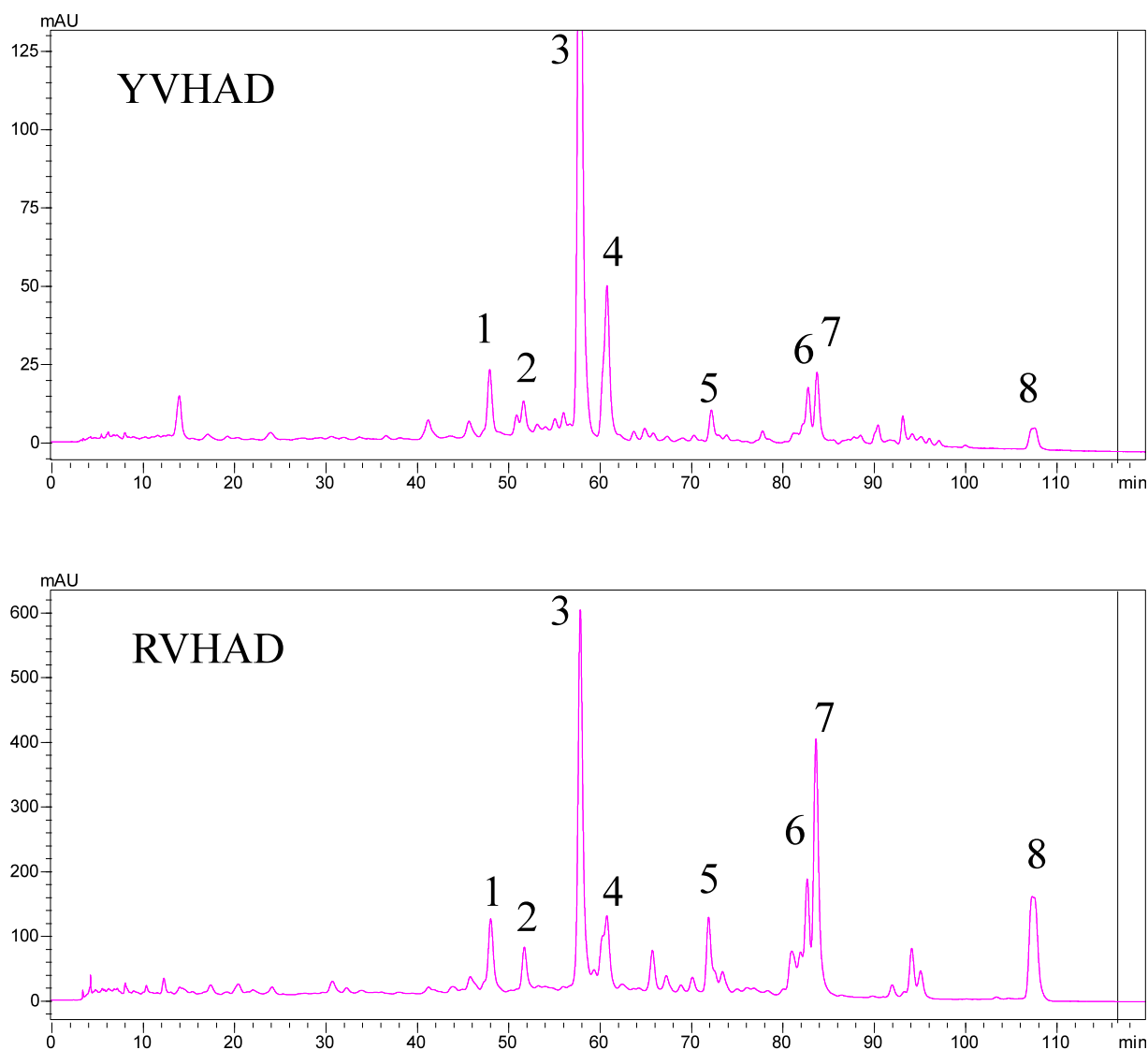


**Figure 2.** HPLC–DAD–MS analysis of carotenoids in fruit (*Bactris gasipaes*) fruit peels (column C<sub>30</sub>). YVHAD: Yellow variety, hot air-dried, cooked. RVHAD: Red variety, hot air-dried, cooked. Peak numbers correspond to the compound numbers in Table 2.

peach palm fruit peel flours (red and yellow varieties) obtained by hot-air dehydration in comparison to freeze-drying methodology and study their carotenoid and phenolic composition. With these results, one sample was chosen to formulate a carotenoid-rich emulsion-based delivery system through ultrasound-assisted emulsification and using a response surface as a process optimization methodology.

## RESULTS AND DISCUSSION

**Physicochemical Characterization of Peach Palm Fruit Peel Flours.** The physicochemical characterization of flours obtained from both varieties (yellow and red) of *B. gasipaes* peels by drying (raw, freeze-drying and cooked, hot air-drying) is shown in Table 1. *B. gasipaes* fruit is consumed

**Table 3. Phenolic Composition of Peach Palm Fruit (*Bactris gasipaes*) Peel Flours Obtained by Freeze Drying<sup>a</sup>**

no.	RT (min)	compound	[M–H] <sup>–</sup>	UV–vis $\lambda$ (nm)	YVFD (%)	RVFD (%)
9	2.3	quinic acid	191	220, 270	1.29 ± 0.18	2.75 ± 0.36
10	2.6	feruloylquinic acid	367	221, 271	29.78 ± 0.91	32.29 ± 0.42
11	5.9	cinnamoyl glucoside	309	283	0.57 ± 0.03	nd
12	7.6	procyanidin dimer, isomer I	577	216, 277	42.59 ± 0.75	39.74 ± 0.40
13	8.4	procyanidin dimer, isomer II	577	216, 277	0.74 ± 0.02	0.92 ± 0.01
14	10.9	maloyl caffeoylshikimic acid	451	270, 320	2.35 ± 0.21	6.61 ± 0.06
15	14.3	apigenin 6,8-di-C-hexoside (vicenin-2)	593	270, 335	2.69 ± 0.33	2.94 ± 0.13
16	15.7	neoschaftoside	563	270, 335	2.36 ± 0.46	1.86 ± 0.05
17	16.1	isoschaftoside	563	270, 334	5.21 ± 0.09	5.86 ± 0.16
18	16.3	apigenin 6-C hexoside 8-C-pentoside (shaftoside)	563	270, 334	2.12 ± 0.27	2.85 ± 0.19
19	17.5	vicenin-1	563	270, 334	2.37 ± 0.10	0.79 ± 0.03
20	18.3	apigenin-8-C-hexoside (Vitexin)	431	271, 335	0.47 ± 0.03	0.37 ± 0.05
21	18.5	apigenin-6-C-hexoside (isovitexin)	431	270, 334	3.32 ± 0.17	2.56 ± 0.16
22	27.3	luteolin	285	252, 335	0.54 ± 0.01	0.20 ± 0.00
23	31.2	apigenin	269	265, 335	3.60 ± 0.49	0.27 ± 0.01

<sup>a</sup>RT = retention time in C<sub>18</sub> HPLC column. YVFD = Yellow variety, freeze-dried, raw; RVFD = Red variety, freeze-dried, raw. nd = not detected.

after cooking; however, freeze-dried fruit peels were characterized to assess the effect of thermal treatment. The water activity (*A<sub>w</sub>*) values were similar between the varieties and slightly higher on the samples obtained by hot air-drying. All the samples exhibited *A<sub>w</sub>* values below the accepted maximum (0.5) to reduce the risk of microbial food spoilage.<sup>20</sup> The flours from the yellow variety were slightly more acidic than the red ones, as seen from the pH and acidity values. Proximal analysis of fruit peel flours showed that they are a source of carbohydrates, lipids, and proteins. Interestingly, the red variety showed higher protein, lipid, and crude fiber contents and lower carbohydrate content. Arecaceae palm fruits are rich in lipids, which are mainly located in pulp (7.70–61.70% oil content) and the hard kernel (11.50–23.50% oil content)<sup>21</sup> showing great potential for their use in the food, cosmetic, pharmaceutical, or biofuel industries. Also, the protein content of epicarp flours of *B. gasipaes* fruits is like those of other Arecaceae fruits, such as acai (*Euterpe oleraceae*) and buriti (*Mauritia flexuosa*).<sup>22</sup> The protein content of *B. gasipaes* epicarp flours is higher than that of the mango<sup>23</sup> or banana epicarp<sup>24</sup> flours, showing a potential to be used as a food additive.

The results obtained by tristimulus colorimetry (Table 1) showed lower values in lightness (*L*<sup>\*</sup>) and chroma (*C<sub>ab</sub>*<sup>\*</sup>) in the yellow variety epicarp flours, which is in agreement with the intense red color of this variety. Regarding the drying method, *L*<sup>\*</sup> and *C<sub>ab</sub>*<sup>\*</sup> values were lower in cooked peel flours, likely due to the decomposition of carotenoids by thermal treatment. The *a*<sup>\*</sup> values for red variety flours were higher than yellow variety flours; a significant effect of the hot-air drying technique was observed in the *a*<sup>\*</sup> and *b*<sup>\*</sup> values by temperature effect.

The *h<sub>ab</sub>* values vary between 69.62 and 86.24, indicating that all of these samples are in the first quadrant (+*a*<sup>\*</sup> and +*b*<sup>\*</sup>). The color index (IC<sup>\*</sup>) values showed significant differences between varieties and among the two drying techniques, confirming the effect of the temperature on the color. These color differences are quantified by  $\Delta E^*$  values that differ between the yellow variety (32.05 ± 1.42) and the red variety (44.69 ± 2.37).

**Carotenoid and Phenolic Compositions of Peach Palm Fruit Peel Flours.** Total carotenoid content and provitamin A data are reported in Table 1. Significant

differences were found among the two varieties, with a higher carotenoid content on the red variety than on the yellow one in both drying methods (ca. 11-fold ratio). Regarding the thermal treatment in hot air-dried cooked fruit peels, an increase in the carotenoid content of 1.7-fold was found compared to the freeze-dried peels. Similar data were reported by Rojas-Garbanzo et al.<sup>25</sup> in *B. gasipaes* fruit pulp, where the thermal effect favored the formation of all-*trans*- $\alpha$ -cryptoxanthin and 15-*cis*- $\beta$ -carotene after cooking. The temperature could alter the cell membrane and protein-carotenoid complexes, making carotenoids more accessible to extraction.<sup>26</sup> The provitamin A data followed the same behavior as the carotenoid content, suggesting that this activity is related to the carotenoid composition of this peel fruit.

The carotenoid compositions of four *B. gasipaes* peel flours are shown in Table 2, and the total ion chromatograms obtained by HPLC-PDA-MS of yellow and red variety peels, cooked and hot air-dried (YVHAD and RVHAD, respectively), are shown in Figure 2. Eighth carotenoid compounds were identified in both varieties, finding only differences in the quantitative data. The main carotenoids in both varieties were  $\beta$ -carotene,  $\gamma$ -carotene, and 13-*cis*- $\beta$ -carotene; *Z*- $\gamma$ -carotene was a main component in RVHAD and 9-*cis*- $\beta$ -carotene in YVHAD. The temperature allowed the increase in the amount of all carotenoids (ca. 2-fold), which was more notable for lycopene in both varieties.

These data agreed with those previously published,<sup>7</sup> where the carotenoids were identified only by HPLC-PDA from the cooked peel (different varieties). The main differences of this work compared to previously reported data were that violaxanthin, lutein, and zeaxanthin were not detected, whereas additional carotenoids such as  $\delta$ -carotene, *Z*- $\gamma$ -carotene,  $\gamma$ -carotene, and lycopene were identified. Menezes Silva et al.<sup>8</sup> analyzed the carotenoid composition of cooked freeze-dried *B. gasipaes* peels of the orange variety from Brazil, and the composition was similar to that of the RVHAD sample. The vitamin A value of the red variety (raw or cooked, 20.90 ± 0.54 and 33.10 ± 0.83, respectively) was in the range of those reported for the orange variety from Brazil, which varied from 25.14 ± 2.06 to 38.22 ± 2.15  $\mu$ g RAE/g, depending on the extraction method.<sup>8</sup>

These results confirmed the potential of the *B. gasipaes* peel as a source of carotenoids and provitamin A activity, according

**Table 4. Experimental Design Matrix with Experimental and Predicted Results for each of the Response Variables in the Optimization of the Carotenoid-Rich Emulsion Development**

runs	oil (%) $X_1$	emulsifiers (%) $X_2$	power (W) $X_3$	time (min) $X_4$	$Y_1$ : carotenoid content ( $\mu\text{g/g}$ )		$Y_2$ : emulsion droplet size (nm)		$Y_3$ : PDI <sup>a</sup>	
					experimental	predicted	experimental	predicted	experimental	predicted
1	0	0	0	2	53.31	52.75	622.46	620.77	0.258	0.255
2	-1	1	1	-1	51.98	51.10	517.13	520.25	0.220	0.228
3	0	2	0	0	50.12	51.18	641.20	640.54	0.247	0.234
4	0	0	0	-2	47.65	48.68	668.26	667.56	0.388	0.376
5	-1	-1	1	-1	43.01	43.39	550.06	551.32	0.289	0.310
6	0	0	0	0	52.04	51.38	646.63	648.48	0.179	0.176
7	1	-1	-1	1	48.55	49.09	749.56	747.93	0.239	0.235
8	-1	-1	1	1	51.39	51.29	525.63	530.66	0.392	0.398
9	1	1	-1	1	44.93	44.47	770.53	770.21	0.332	0.322
10	1	-1	1	1	67.61	68.18	502.23	500.94	0.170	0.179
11	-1	1	-1	1	42.37	42.77	712.50	715.16	0.165	0.164
12	1	-1	1	-1	59.93	59.19	572.13	570.95	0.264	0.269
13	0	0	0	0	51.19	51.38	646.66	648.48	0.130	0.176
14	0	0	-2	0	37.09	37.04	856.00	855.65	0.244	0.267
15	0	0	2	0	59.03	59.55	439.03	436.97	0.281	0.243
16	0	0	0	0	51.38	51.38	648.16	648.48	0.202	0.176
17	2	0	0	0	62.64	62.87	686.90	692.05	0.415	0.399
18	1	1	1	1	63.96	63.69	549.76	549.56	0.200	0.224
19	0	0	0	0	51.17	51.38	653.76	648.48	0.199	0.176
20	-1	1	-1	-1	48.33	47.68	689.73	691.95	0.195	0.197
21	-1	1	1	1	53.29	53.18	523.93	524.16	0.287	0.290
22	-1	-1	-1	1	40.83	41	746.66	748.01	0.236	0.230
23	-2	0	0	0	45.12	45.36	624.93	617.37	0.282	0.282
24	1	1	1	-1	60.78	60.52	595.43	595.02	0.323	0.339
25	1	-1	-1	-1	47.06	47.09	797.93	798.63	0.409	0.418
26	-1	-1	-1	-1	40.17	40.09	747.66	749.35	0.256	0.236
27	0	0	0	0	51.09	51.38	647.16	648.48	0.172	0.176
28	1	1	-1	-1	48.54	48.30	799.90	796.35	0.534	0.531
29	0	-2	0	0	48.67	48.08	651.06	649.32	0.232	0.229

<sup>a</sup>PDI = polydispersity index.

to the classification proposed by Britton and Khachik<sup>27</sup> who stated a 20  $\mu\text{g/g}$  minimum carotenoid content for this activity and for any matrix to be considered as having a very high carotenoid content.

**Phenolic Composition of Peach Palm Fruit Peel Flours.** The phenolic composition of *B. gasipaes* peel flour was studied to give added value to this byproduct. Data reported in Table 1 showed that the red variety's total phenolic content (TPC) was significantly higher than the yellow variety in both drying methods. The flours of both varieties of peels, obtained by freeze-drying, exhibited the highest TPC values, showing the effect of thermal treatment on phenolic compound stability. The phenolic composition of freeze-dried *B. gasipaes* peels was analyzed by HPLC/PDA-ESI/MS, and the results are summarized in Table 3. Procyanidin dimer (isomer I), feruloyl quinic acid, isoschaftoside, apigenin, isovitexin (apigenin-6-C-hexoside), vienin-2 (apigenin 6,8-di-C-hexoside), and maloyl caffeoyl shikimic acid were identified as major constituents in both varieties. Small differences were found; cinnamoyl glucoside was predominant in the yellow variety, while vicenin-2 was predominant in the red variety. The HPLC profile of both samples is shown in the Supporting Information (Figure 1S). The apigenin C-glycosides and the maloyl caffeoylshikimic acid were also detected in the cooked pulp of orange and yellow *B. gasipaes* fruits.<sup>10</sup> Concerning the biological potential of these flavonoids, antimelanogenic and

antineuroinflammatory activities and hepatoprotective effects have been reported previously for the schaftoside.<sup>10</sup>

**Development of Carotenoid-Rich Emulsion-Based Delivery System.** Based on the above-mentioned results, the red variety was selected to develop a carotenoid-rich emulsion as a source of Provitamin A to fortify foods. Thus, sunflower commercial oil was chosen to obtain a carotenoid-rich extract as an alternative for fortifying it with Provitamin A. Sunflower oil loses a significant amount of its carotenoid and xanthophyll content during industrial refining, bleaching, and/or deodorizing. The maximum reduction occurs during blanching, where around 77% of the carotenoids are lost, and in the subsequent deodorization stage, the carotenoids are further eliminated.<sup>28</sup>

The extraction of RVHAD flour with sunflower oil assisted by homogenization with Ultraturrax exhibited the highest carotenoid content (in comparison to other extraction techniques such as ultrasound assisted, Soxhlet extraction, and maceration, data not shown) of  $334.41 \pm 2.06 \mu\text{g/g}$ , with a yield of 40.16%, and a peroxide index of  $3.15 \text{ meq} \pm 0.02 \text{ meq O}_2/\text{kg}$  at  $30 \pm 2 \text{ }^\circ\text{C}$ . The color difference between the *B. gasipaes* carotenoid-rich sunflower oil ( $\Delta E^* = 88.04 \pm 0.03$ ) and the original sunflower oil confirmed its enrichment with the carotenoid pigments extracted from peach palm epicarp flour (*Bactris gasipaes*). According to the results, it is evident that sunflower oil is a suitable solvent in the green extraction of

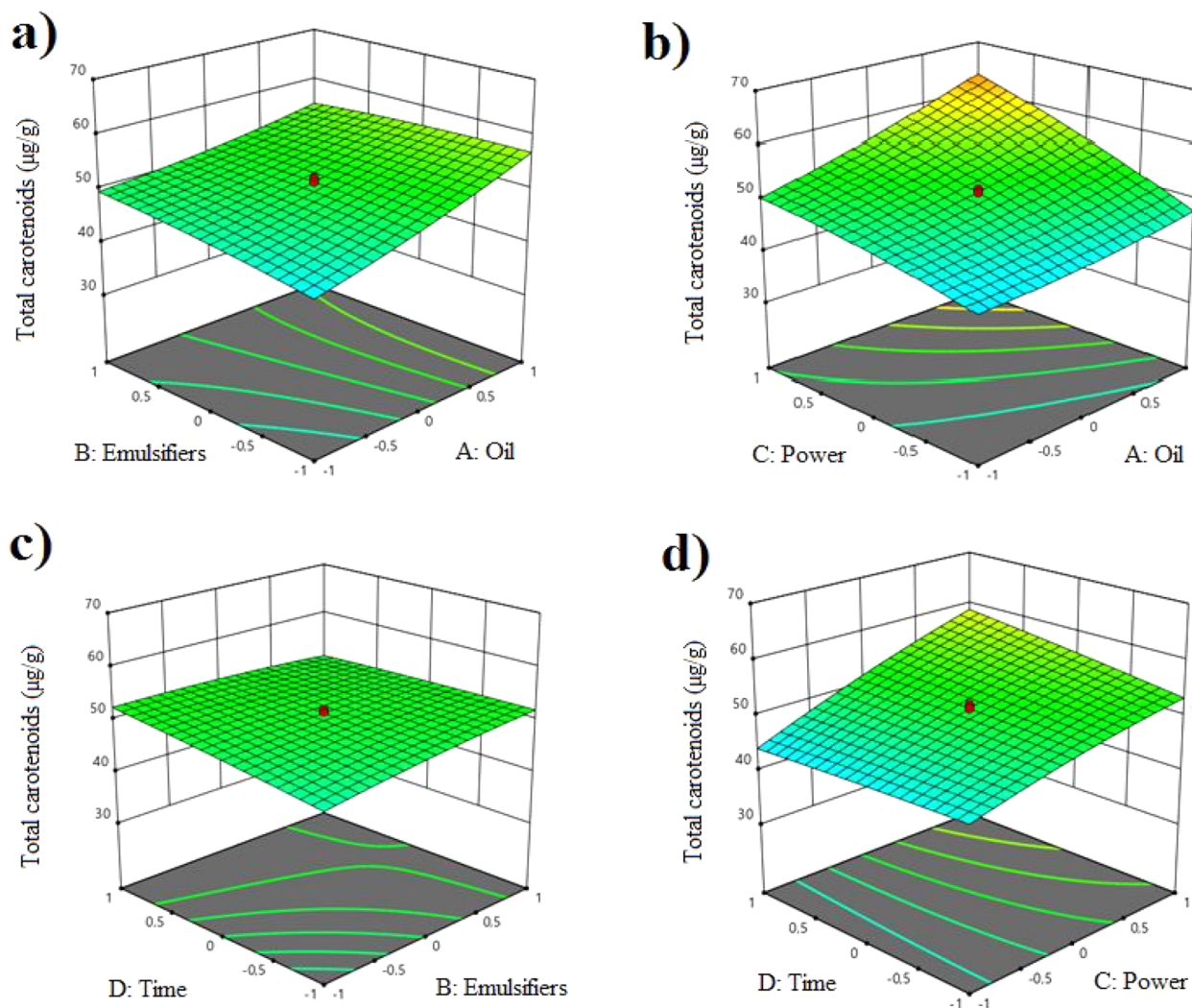


**Figure 3.** Three-dimensional plots of CCD-RSM showing the processing variable effects on the carotenoid content. Total carotenoid content vs (a) oil and emulsifier contents, (b) oil content and ultrasonic power, (c) emulsifier content and ultrasonic time, and (d) ultrasonic power and time.

carotenoid pigments present in peach palm fruits, as has been reported in previous studies.<sup>29</sup>

Response surface methodology (RSM) is a statistical methodology commonly used to design experiments and formulate food or pharmaceutical products; among other things, it has been used to develop emulsion-based delivery systems for carotenoids.<sup>30</sup> Thus, the variables selected for applying this model were carotenoid-rich oil (%) used as the oil phase in the emulsion and a source of provitamin A carotenoids from *B. gasipaes* peel flour; emulsifiers (%), amphiphilic molecules that assemble at the interface of oil/water phase boundaries, reducing the surface tension and thereby resisting phase separation of the dispersed droplets;<sup>31</sup> ultrasonic power (W); and time (min) of ultrasonic power to obtain the emulsion. The response variables were the carotenoid content ( $\mu\text{g/g}$ ), droplet size (nm), and polydispersity index (PDI) of emulsions.

**Effect on the Carotenoid Content.** This variable was included because it is directly related to the provitamin A activity, which is the target of this work. The carotenoid content in the emulsions ranged from 37.09 to 67.61  $\mu\text{g/g}$ , as seen in Table 4. Recently, an O/W emulsion using carotenoid-

rich sunflower oil from the peach palm mesocarp was characterized, finding a carotenoid content of  $1.256 \pm 0.073$   $\mu\text{g/g}$ ,<sup>15</sup> lower than that obtained in this study. This difference may be due to different factors but predominantly to the fact that epicarp exhibits a higher carotenoid content than *B. gasipaes* mesocarp.<sup>5</sup>

The ANOVA analysis of the response variables is presented in Table 1S. The model had a significance level of  $p < 0.0001$ , which indicates that the model manages to explain the variations within the system. All independent factors presented a significant difference ( $p < 0.0001$ ) in the carotenoid content, as did the interaction factors ( $X_1X_2$ ,  $X_1X_3$ ,  $X_2X_4$ ,  $X_3X_4$ ) and the quadratic effect factors ( $X_1^2$ ,  $X_2^2$ ,  $X_3^2$ ). Regarding carotenoid content, the lack of fit was not significant ( $p > 0.05$ ),  $R^2 = 0.9954$ ,  $\text{adj } R^2 = 0.9908$ ,  $\text{pred } R^2 = 0.9751$ ,  $\text{CV} = 1.39\%$ , and  $\text{adeq precision} = 61.456$ , evidencing that the model presented a good fit to the regression. Given the above, the final model to predict the carotenoid content was represented by the polynomial equation presented below (eq 1):

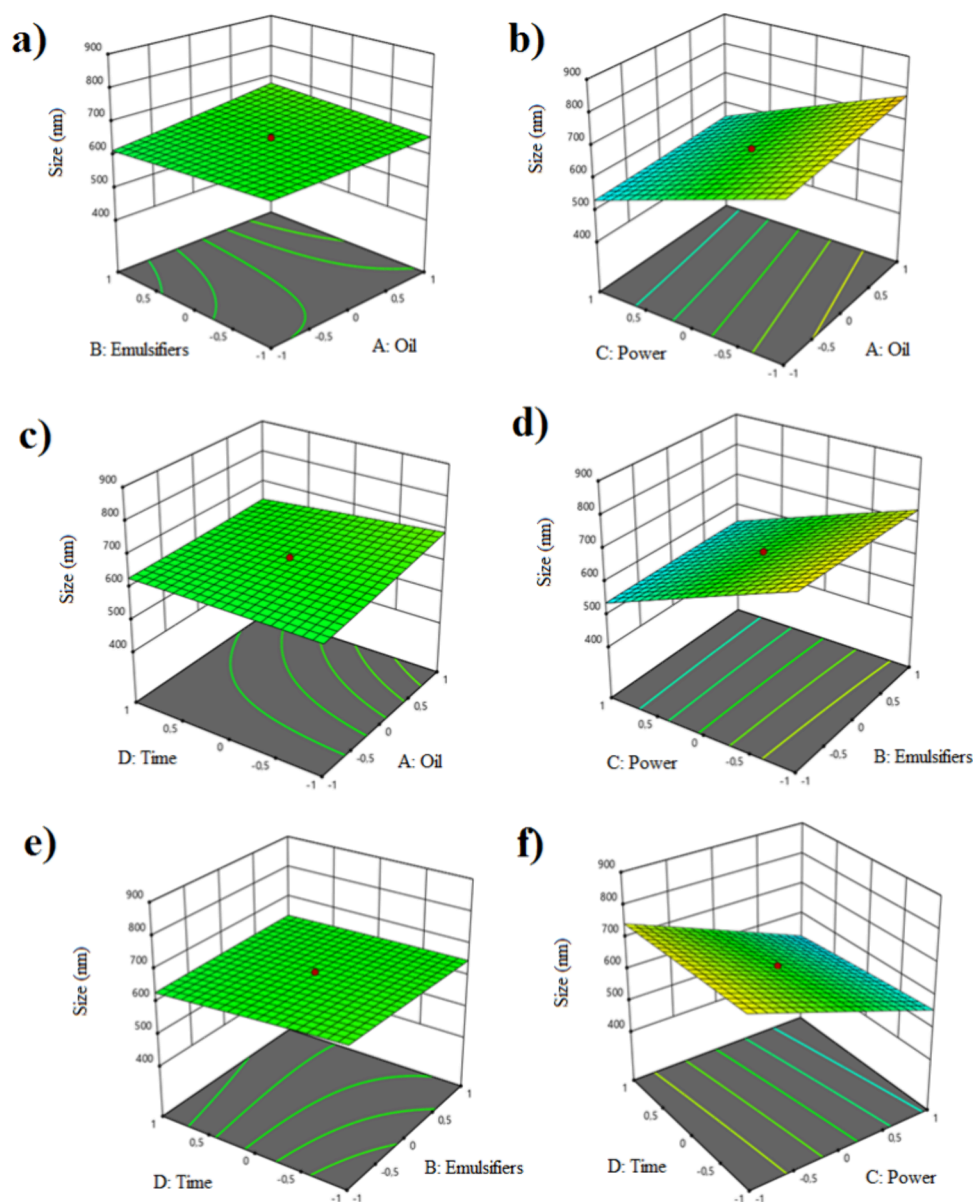


**Figure 4.** Three-dimensional plots of CCD-RSM showing the effects of ultrasonic emulsification conditions on the droplet size. Droplet size vs (a) oil and emulsifier contents, (b) oil content and ultrasonic power, (c) oil content and ultrasonic time, (d) emulsifier content and ultrasonic power, (e) emulsifier content and ultrasonic time, and (f) ultrasonic power and time.

$$\begin{aligned}
 Y_1 = & 51.38 - 4.38X_1 + 0.7732X_2 + 5.63X_3 + 1.02X_4 \\
 & - 1.59X_1 \times X_2 + 2.20X_1 \times X_3 - 1.46X_2 \times X_4 \\
 & + 1.75X_3 \times X_4 + 0.6834X_1^2 - 0.438X_2^2 - 0.771X_3^2
 \end{aligned}
 \quad (1)$$

The previous equation shows how independently the effect of ultrasonic power ( $X_3$ ), the interaction of oil ( $X_1$ ) and ultrasonic power ( $X_3$ ), and the square effect of oil ( $X_1^2$ ) increase the concentration of carotenoids, while the interaction of oil ( $X_1$ ) and emulsifiers ( $X_2$ ) reduces the concentration of carotenoids. The response surfaces related to the carotenoid content in the developed emulsions are shown in Figure 3a–d, where the interaction and quadratic effects of the emulsifier (%), oil content (%), ultrasonic power, and time on the carotenoid content are shown. A significant increase in carotenoid content was observed when the ultrasonic power was increased from 120 to 480 W. This can be explained by the

rise in the mass transfer coefficient between the carotenoid pigments and the oil due to the waves produced by cavitation that allow their release from the matrix<sup>18</sup> that generate an increase in the diffusion speed and a decrease in viscosity.<sup>32</sup> However, at 600 W of power, there was a reduction in carotenoids compared to the value obtained at 480 W. High power values can generate the collapse of the carotenoid cavitation bubbles due to strong shock waves causing an increase in the concentration of free radicals that trigger oxidation and degradation reactions of carotenoids.<sup>33</sup>

On the other hand, the interaction of oil (%) with the increase in the content of emulsifiers can reduce the carotenoid content due to the increase in viscosity, which decreases the release of carotenoid pigments from the matrix. Figure 3c and d show the response surfaces generated by the significant effect of emulsifier content and time and the impact of ultrasonic power and time on the carotenoid content, respectively. It is observed that the greater the emulsifier amount, the greater the

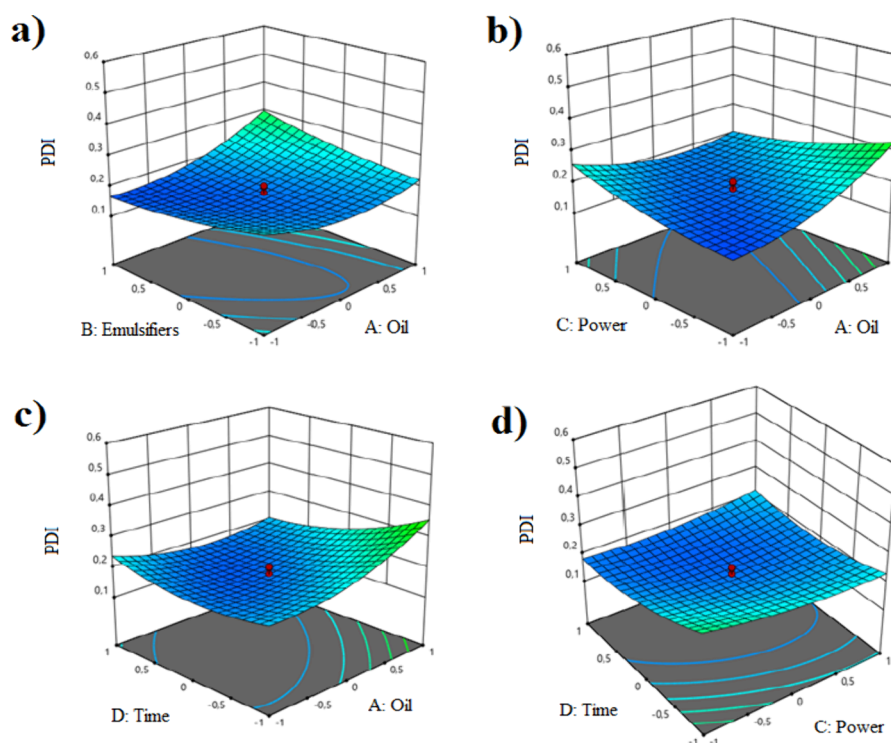


**Figure 5.** Three-dimensional plots of CCD-RSM showing the effects of ultrasonic emulsification conditions on the PDI. Polydispersity index (PDI) vs (a) oil and emulsifier contents, (b) oil content and ultrasonic power, (c) oil content and ultrasonic time, and (d) ultrasonic power and time.

viscosity, affecting the concentration of the carotenoids. Also, the longer the time, the lower the concentration, since the viscosity increases, making releasing the pigments from the matrix difficult. By gradually increasing the time and ultrasonic power from 120 to 480 W, the relative force in the cavitation core is greater, allowing the release of bioactive compounds from the matrix caused by the increase in mass transfer.<sup>17,19</sup>

**Effect on the Droplet Size.** Considering the relevance of the droplet size to emulsion stability, appearance, and taste, this parameter was also included as one of the response variables in the experimental statistical design. The droplet size of the emulsions ranged between 439 and 856 nm, as seen in Table 4. These values are in the range of mini (nano) emulsions; as the value is lower, the emulsion becomes more stable.

The ANOVA analysis for this response variable (Table 1S) indicates that the model, the independent variables, and their interaction factors presented a significant difference ( $p < 0.05$ ). For droplet size, the lack of fit was not significant ( $p > 0.05$ ), with  $R^2 = 0.9993$ ,  $\text{adj } R^2 = 0.9986$ ,  $\text{pred } R^2 = 0.9964$ ,  $\text{CV} = 0.59\%$ , and  $\text{adeq precision} = 152.541$ , evidencing that the model presented a good regression fit. Given the above, the final model for droplet size was represented by the polynomial equation presented below (eq 2):

$$Y_2 = 648.48 + 18.67X_1 - 2.20X_2 - 104.67X_3 - 11.70X_4 + 13.78X_1 \times X_2 - 7.41X_1 \times X_3 - 12.41X_1 \times X_4 + 6.59X_2 \times X_3 + 6.14X_2 \times X_4 - 4.83X_3 \times X_4 \quad (2)$$

This equation shows that the highest coefficient independently corresponds to the power variable ( $X_3$ ) with a negative value. In contrast, the oil interaction ( $X_1$ ) and emulsifier ( $X_2$ ) increase the droplet size in the emulsion. This indicates that the droplet size decreased if the ultrasonic power and time increased, as reported in the literature.<sup>32</sup>

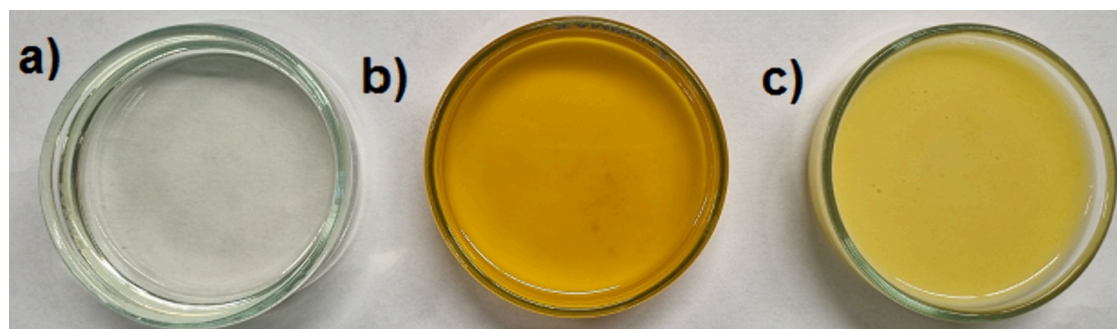
Figure 4a and b present the response surfaces generated by the emulsifier and oil content effects and the ultrasonic power and oil content effects on the droplet size, respectively. The oil content and emulsifiers increase the drop size due to the increase in viscosity, while the increase in ultrasonic power decreases the drop size. The decrease in droplet size when applying ultrasound is due to the cavitation pressure generated by acoustic waves that favor the dispersion of particles.<sup>19</sup>

Figure 4c and d show the effect of time and oil content and the effect of ultrasonic power and emulsifiers on the droplet size, respectively. It was observed that the ultrasonic time reduces the droplet size due to a decrease in viscosity, while the increase in oil increases the droplet size due to the greater oil phase content in the emulsion. Figure 4d shows that a reduction in droplet size occurs at higher emulsifier content, possibly due to the hydrolysis of xanthan gum and soy lecithin because of ultrasound. Figure 4e and f show the effect of emulsifier content and ultrasonic time and the effect of ultrasonic power and time on droplet size, respectively.

Ultrasonic time and emulsifiers (%) can reduce the droplet size, considering that the longer the ultrasonic time, the greater the hydrolysis of the emulsifiers is achieved, which influences a reduction in viscosity. This fact is important for emulsions enriched with bioactive compounds because the decrease in droplet size improves the bioaccessibility of carotenoid pigments.<sup>15,34</sup>

**Effect on the Polydispersity Index (PDI).** This parameter is also related to emulsion stability. Lower values of PDI (0.08–0.7) are desirable for uniform distribution, stability, and high dispersion, which is positive because it promotes no phase separation during storage. In contrast, higher PDI values ( $>0.7$ ) indicate that the sample has a very broad particle size distribution quality.<sup>31</sup> The PDI values for emulsions exhibited values between 0.130 and 0.534 (Table 4). According to the





**Figure 6.** (a) Sunflower oil, (b) oil phase (carotenoid-rich from the peach palm epicarp sunflower oil), (c) optimized emulsion.

**Table 5. Physicochemical Characterization of the Optimized Emulsion during Storage<sup>a</sup>**

variable	day 0	day 7	day 21	day 35
phase separation	stable	stable	stable	stable
pH	6.17 ± 0.03 <sup>a</sup>	6.14 ± 0.02 <sup>a</sup>	6.13 ± 0.04 <sup>a</sup>	6.11 ± 0.08 <sup>a</sup>
conductivity (μs/cm)	102.15 ± 0.62 <sup>a</sup>	102.10 ± 0.67 <sup>a</sup>	102.08 ± 0.73 <sup>a</sup>	102.10 ± 0.69 <sup>a</sup>
viscosity (cP)	23.24 ± 0.67 <sup>a</sup>	23.29 ± 0.68 <sup>a</sup>	23.31 ± 0.69 <sup>a</sup>	23.33 ± 0.71 <sup>a</sup>
zeta potential (mV)	-32.26 ± 1.61 <sup>a</sup>	-32.24 ± 1.62 <sup>a</sup>	-32.22 ± 1.65 <sup>a</sup>	-32.20 ± 1.67 <sup>a</sup>
droplet size (nm)	502.23 ± 3.83 <sup>b</sup>	491.52 ± 2.94 <sup>c</sup>	502.46 ± 3.72 <sup>b</sup>	517.38 ± 3.37 <sup>a</sup>
polydispersity index (PDI)	0.170 ± 0.01 <sup>a</sup>	0.168 ± 0.01 <sup>a</sup>	0.171 ± 0.01 <sup>a</sup>	0.174 ± 0.01 <sup>a</sup>
turbidity (NTU)	74.53 ± 0.78 <sup>a</sup>	74.50 ± 0.75 <sup>a</sup>	68.76 ± 0.38 <sup>b</sup>	63.07 ± 0.36 <sup>c</sup>
carotenoid content (μg/g)	67.61 ± 0.83 <sup>a</sup>	64.33 ± 0.56 <sup>b</sup>	60.04 ± 0.22 <sup>c</sup>	58.55 ± 0.37 <sup>d</sup>
color parameters				
<i>L</i> *	80.22 ± 0.03 <sup>c</sup>	82.93 ± 0.09 <sup>ab</sup>	83.36 ± 0.06 <sup>b</sup>	84.57 ± 0.07 <sup>a</sup>
<i>a</i> *	13.89 ± 0.04 <sup>a</sup>	13.54 ± 0.05 <sup>ab</sup>	12.96 ± 0.03 <sup>bc</sup>	11.94 ± 0.04 <sup>c</sup>
<i>b</i> *	46.53 ± 0.03 <sup>a</sup>	44.91 ± 0.04 <sup>b</sup>	42.95 ± 0.06 <sup>bc</sup>	41.67 ± 0.07 <sup>c</sup>
Δ <i>E</i> *		3.17 ± 0.05 <sup>c</sup>	4.85 ± 0.04 <sup>b</sup>	6.80 ± 0.05 <sup>a</sup>

<sup>a</sup>Temperature of storage: 30 ± 2 °C. According to Tukey's multiple range test, values in the same column followed by the same letter are not significantly different ( $p > 0.05$ ).

ANOVA analysis (Table 1S), the experimentation factors ( $X_1$ ,  $X_4$ ), the interaction factors ( $X_1X_2$ ,  $X_1X_3$ ,  $X_1X_4$ ), and all the quadratic factors showed significant differences ( $p < 0.05$ ) over the polydispersity index. The lack of fit was not significant ( $p > 0.05$ ), with  $R^2 = 0.9652$ ,  $\text{adj } R^2 = 0.9304$ ,  $\text{pred } R^2 = 0.8589$ ,  $\text{CV} = 9\%$ , and  $\text{adeq precision} = 21.228$ , evidencing that the model presented a good regression fit. Given the above, the final model for the polydispersity index was represented by the polynomial equation presented below (eq 3):

$$\begin{aligned}
 Y_3 = & 0.1767 + 0.0291X_1 - 0.0303X_4 + 0.0382X_1 \times X_2 \\
 & - 0.0558X_1 \times X_3 - 0.0444X_1 \times X_4 + 0.0235X_3 \times X_4 \\
 & + 0.0411X_1^2 + 0.0138X_2^2 + 0.0196X_3^2 + 0.0348X_4^2
 \end{aligned}
 \quad (3)$$

The previous equation shows that the highest coefficient occurs in oil ( $X_1$ ) and power ( $X_3$ ) interactions with a negative value. The interaction of these factors produces a lower PDI value, and the oil quadratic value ( $X_1^2$ ) increases the PDI value. Figure 5a and b show the response surfaces generated by the emulsifier and oil content and the effect of the ultrasonic power and oil on the polydispersity index, respectively. It is observed that the lower the oil and emulsifier content, the lower the PDI value due to the decrease in viscosity and the variation in droplet size distribution caused by homogenization. In turn, at higher ultrasonic power and lower oil content (Figure 5b), an adequate dispersion of the droplets is observed, which reduces the PDI value. Figure 5c and d show the response surfaces generated by the effect of oil content and

time and the effect of ultrasonic power and time on the polydispersity index, respectively. Figure 5c shows that the shorter the ultrasonic time and the higher the oil concentration, the more the PDI increased. Figure 5d showed that the higher the ultrasonic time and power, the more the PDI decreased. In this sense, the oil content can increase the PDI, but the longer the ultrasonic time, the more the PDI is reduced due to the greater exposure to cavitation effects.<sup>19,32</sup>

Finally, the optimization of the emulsification process showed that the optimal conditions allowed the highest carotenoid content of 67.61 μg/g and a provitamin A content of 3.23 ± 0.56 μg RAE/g, with an emulsion droplet size of 502.23 nm and PDI of 0.170 corresponding to 25% carotenoid-rich oil, 1.25% emulsifiers, 480 W ultrasound power, and a time of 5 min. The validations of the optimization conditions at the experimental level reported values of 67.49 μg/g for the carotenoid content, a droplet size of 501.96 nm, and a PDI of 0.169. These data did not show significant differences ( $p > 0.05$ ) with the theoretical values, indicating that the experimental values adjusted to the theoretical model. Additionally, the provitamin A content on the optimized emulsion was 3.23 ± 0.56 μg of RAE/g, confirming its potential as an additive for food fortification. The carotenoid-rich sunflower oil used and the optimized emulsion are shown in Figure 6.

**Stability Study of a Carotenoid-Rich Emulsion-Based Delivery System.** In this work, the emulsion is a vehicle for delivering *B. gasipaes* peel carotenoids as bioactive compounds. To the extent the emulsion is more stable, oil-soluble

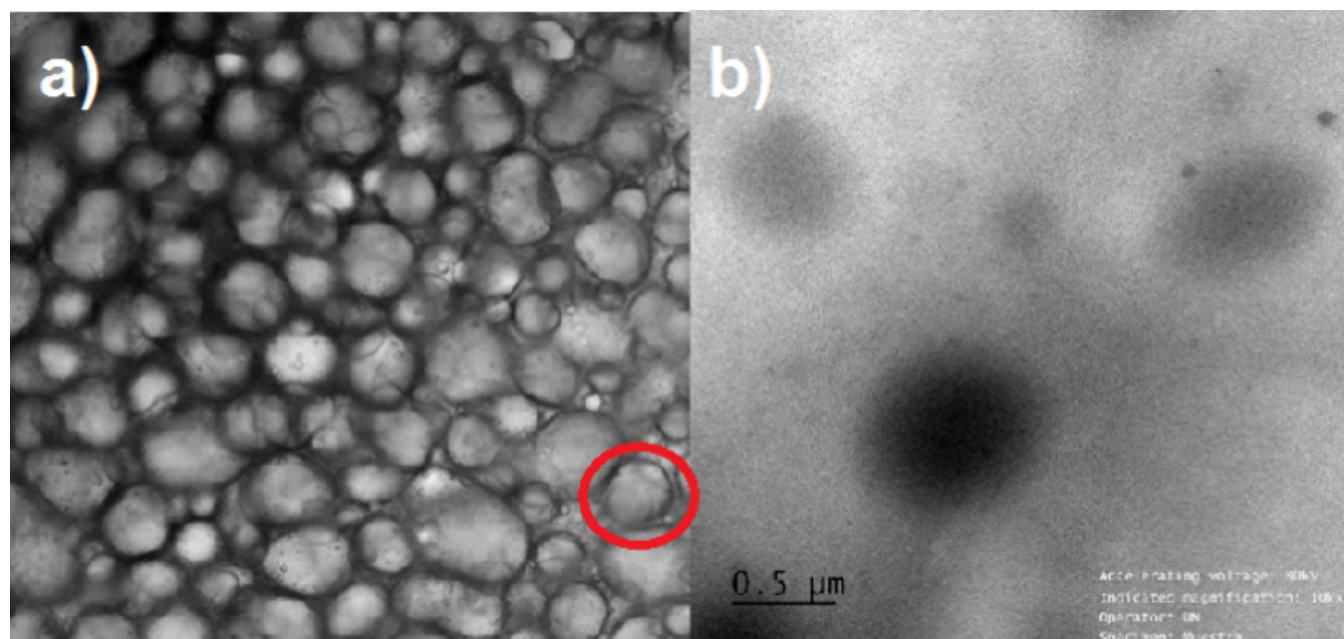


**Figure 7.** Morphology of the optimized emulsion: (a) confocal laser; (b) TEM.

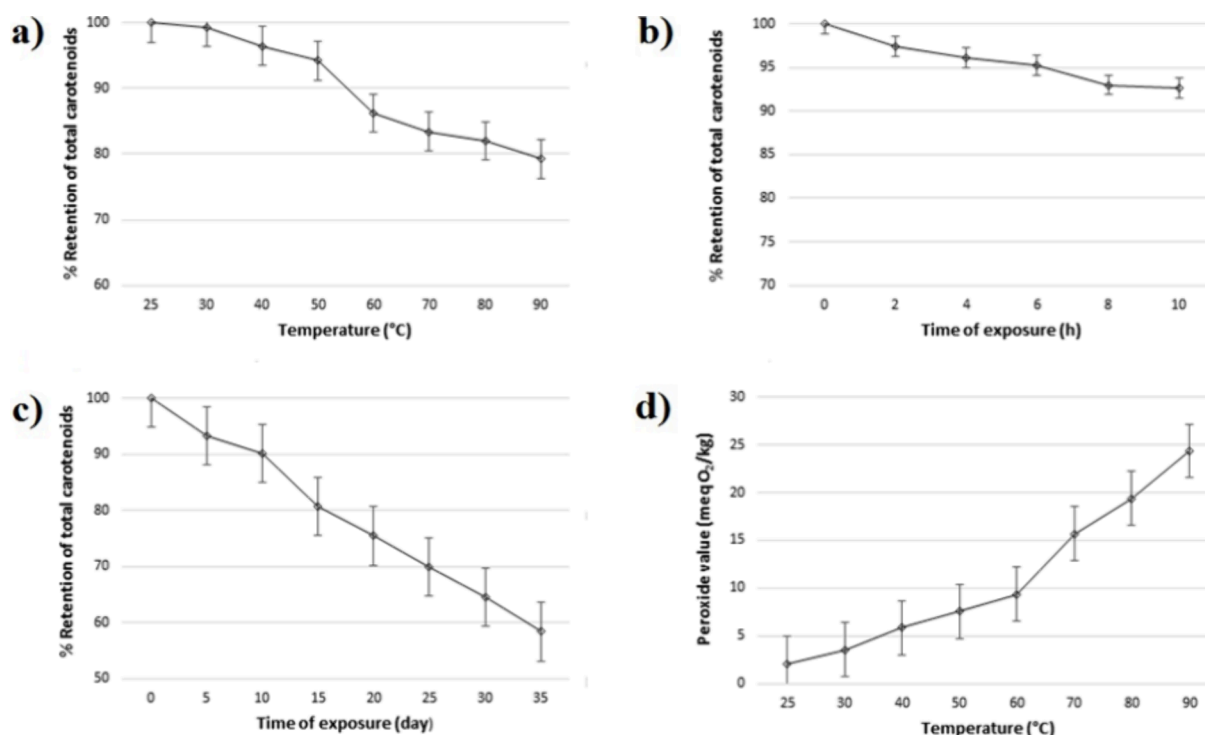


**Figure 8.** Emulsion stability under stress conditions: (a) effect of temperature, (b) effect of exposure to nitrogen, and (c) effect of light on the percentage of carotenoid retention; (d) effect of temperature on the peroxide index.

components will be more efficiently delivered into foods. Table 5 shows the results obtained from the physicochemical characterization of the optimized emulsion during 35 days of storage at  $30 \pm 2$  °C.

The optimized emulsion was stable, without creaming or phase separation during storage and subjection to thermal stress conditions and freeze/thaw cycles; such confirming of pre-emulsification by Ultraturrax combined with ultrasound-assisted emulsification technology and the use of natural emulsifiers allowed adequate physical and chemical stability of

the emulsion. The physicochemical variables, pH, conductivity, viscosity, zeta potential, and PDI did not present significant differences ( $p > 0.05$ ), while droplet size, turbidity, carotenoid content, and CIE- $L^*a^*b^*$  color parameters were significantly affected ( $p < 0.05$ ).

The stability of the pH and conductivity in the emulsion during storage may be associated with the balance between the acidic and basic groups that did not allow the change in the net charge of the droplets, the aqueous phase content, and the contribution of xanthan gum due to its anionic character.<sup>35</sup>

This result may be associated with kinetic stability because of the nonsignificant changes in viscosity and conductivity during emulsion storage.<sup>19</sup> The negative values obtained in the zeta potential measurements are due to the anionic character of the emulsifiers used in the emulsion and indicate the adequate stability of the emulsifying system, allowing the optimized emulsion to be stable during storage.

On the other hand, the results obtained for the droplet size showed a variation from 502.23 to 491.52 nm between days 0 and 7 and a minimum variation from 502.46 to 517.38 nm during days 21 to 35 (Table 5). This decrease in the first days of storage is due to the rearrangement that the particles undergo until equilibrium is achieved after the homogenization process.

Turbidity is a parameter indicative of the number of particles in suspension, and it exhibits a change from 74.53 to 63.07 NTU. This variation is likely associated with the change in droplet size during storage, which increased light dispersion, as reflected by the increase in luminosity  $L^*$  (high luminosity values indicate lighter samples and therefore lower turbidity). These results coincide with those of Singh et al.,<sup>36</sup> who found a decrease in turbidity in the storage of emulsions made by applying ultrasound and soy lecithin and Tween 80 as emulsifiers.

The carotenoid content decreased from 67.61 to 58.55  $\mu\text{g/g}$ , representing a degradation percentage of 13.40% in approximately one month at 30 °C. The reduction of carotenoids during storage can be caused by the peroxidation of the oil, which induces the formation of radicals responsible for the oxidation and isomerization processes of carotenoids.<sup>33,37</sup>

Regarding the surface color of the emulsion, it was observed that luminosity ( $L^*$ ) increased with storage time, while the other color attributes ( $a^*$  and  $b^*$ ) decreased significantly (Table 5). These changes may be associated with the degradation of carotenoid pigments and the reduction in fat globule size during the emulsion homogenization, which increases the reflection area.<sup>38</sup> This fact influenced the values obtained for the color change ( $\Delta E^*$ ; Table 5). These findings suggest that color change is a determining factor in evaluating peroxidation and degradation of carotenoid compounds in emulsions.

Figures 7a,b shows the confocal laser scanning micrographs and transmission electron microscopy (TEM) for the optimized emulsion. The measurements were carried out immediately after preparing the emulsion. The particles of the optimized emulsion were of the order of 0.5  $\mu\text{m}$ . According to the micrographs, the particles presented predominantly spherical and oval shapes, which are characteristic of obtaining nanoemulsions.<sup>35</sup> Spherical droplets with a narrow distribution help to a controlled release over 72 h.<sup>31</sup>

As the carotenoid content is the variable relevant to expressing the provitamin-A activity in the carotenoid-rich emulsion-based delivery system, an additional stability study under stress conditions was performed to evaluate the effect of temperature, nitrogen, and light exposure (Figure 8a–d). The temperature was a critical factor in the carotenoid stability. It was quite stable until 50 °C, and the degradation was more significant after 60 °C, finding the lowest retention value of 79.23% at 90 °C. Nitrogen exposure helps to keep the carotenoid stable; Figure 8b shows that the retention percentage is higher than 90% after 10 h of exposure. In contrast, exposure accelerates the carotenoid degradation, showing a carotenoid retention of 80.09% on day 15, which

drops to 58.36% on day 35 (Figure 8c). Carotenoid degradation is a complex reaction in food, depending on its storage conditions. Thus, light exposure during storage allows isomerization and degradation reactions, and/or elevated temperature exposure can produce autooxidation and photo-oxidation processes, as seen from the results of Figure 8d.<sup>37</sup> At a temperature below 30 °C, the emulsion presented a low peroxide index with values between 2.11–3.56 mequiv  $\text{O}_2/\text{kg}$ , being favorable for the emulsion stability. However, from 50 to 90 °C, the peroxide index increases faster from 7.56 mequiv  $\text{O}_2/\text{kg}$  to 24.34 mequiv  $\text{O}_2/\text{kg}$ .

The increase in the peroxide index may have been accelerated by the presence of reactive species such as alkyl radicals ( $\text{R}-\text{R}'$ ) and peroxy radicals ( $\text{ROO}$ ) that induce the degradation of carotenoids.<sup>33</sup> During the peroxidation process, oxygen initially attacks the terminal unsaturation that most carotenoids, such as  $\beta$ -carotene, have due to the presence of conjugated double bonds, forming  $\beta$ -carotene-5,6-epoxide. Subsequently, oxygen enters the terminal double bond on the other side, producing  $\beta$ -carotene-5,6,5',6'-diepoxide, then rearrangement of the 5,6 to 5,8 epoxide results in  $\beta$ -carotene-5,8-epoxide and  $\beta$ -carotene-5,8,5',8'-diepoxide.<sup>37</sup>

The results obtained in this study are satisfactory because the optimized emulsion obtained a final carotenoid retention percentage of 93% after 10 h of exposure to nitrogen, 79% under a temperature variation of 25 to 90 °C, and 59% after 35 days of exposure to light without the use of encapsulation or the addition of preservatives or synthetic antioxidants after emulsification. Carotenoid-rich emulsion-based delivery systems are more efficient as biofunctional ingredients because their stability and bioaccessibility are better than the lipophilic carotenoids.<sup>39</sup> Additionally, natural emulsifiers such as soy lecithin increase the bioaccessibility of  $\beta$ -carotene by forming mixed micelles with higher solubility.<sup>40</sup>

## CONCLUSIONS

Convection drying of cooked *Bactris gasipaes* peel allows obtaining a food powder (flour) with provitamin A carotenoids, phenolic compounds, fiber, lipids, and proteins, in a higher amount than the lyophilized peel residue. The red variety stands out as being the most significant. Among the two studied varieties, red was the raw material for a carotenoid-rich extract made with sunflower oil. This strategy allowed the transformation of this byproduct into a food additive that can be incorporated into formulations for developing new environmentally friendly nutraceutical products.

The ultrasound-assisted emulsification process and the use of natural emulsifiers (soy lecithin and xanthan gum) allowed for obtaining a carotenoid-rich emulsion that was physically and chemically stable without presenting significant variation in pH, phase separation, conductivity, viscosity, zeta potential, and polydispersity index during storage for 35 days at 30 °C. The optimization of the emulsification process and the use of natural emulsifiers influenced the stability of the emulsion because soy lecithin and xanthan gum could act as physical barriers that helped in part to protect carotenoids. However, the study of stability under stress conditions showed that light could generate photooxidation reactions that significantly affect the provitamin A carotenoids in the emulsion. Thus, packaging is a relevant factor in preserving this activity. Also, the storage temperature must be kept below 30 °C to extend the shelf life of this carotenoid-rich emulsion-based delivery system.

## MATERIALS AND METHODS

**Plant Material.** Ripe peach palm fruits (*Bactris gasipaes*) were acquired in the local markets of Palmira (Valle del Cauca, Colombia) and selected according to their ripeness characteristics (Table 1). Two high-production varieties from southern Colombia were selected: red *cauca* (red variety) and yellow *costeño* (yellow variety; Figure 1). *B. gasipaes* fruits (yellow and red varieties) were washed separately with tap water, followed by immersion in a sanitizing solution (100 ppm sodium hypochlorite) for 10 min. Then, they were divided into two batches, and the first batch was used as a control. Fruit peels were removed, frozen at  $-79 \pm 2$  °C for 24 h in an ultrafreezer (New Brunswick, USA), and then freeze-dried using a Labconco Freezezone 4.5 unit (USA) at a vacuum pressure of 13.30 Pa, to get the samples YVFD and RVFD, from yellow and red varieties, respectively.

The second batch of fruits were cooked ( $90$  °C  $\pm$   $2$  °C, 60 min) and then peeled. The fruit peels (yellow and red varieties) were hot-air-dried (Binder ED 53 UL, GmbH) at  $60$  °C  $\pm$   $2$  °C following the methodology reported by Martínez-Girón et al.<sup>6</sup> to get YVHAD and RVHAD samples, respectively. In both batches, the samples were crushed in an electric mill. They were sieved (Advantech DT-168, Mexico) until obtaining flours with a particle size  $\leq 0.25$  mm; they were then refrigerated in a sterile amber glass jar at  $4$  °C for subsequent analysis.

**Chemicals.** Anhydrous sodium carbonate, ethanol, methanol, hexane, gallic acid, sodium hydroxide, and boric acid were acquired from Sigma-Aldrich (St. Louis, MA, USA). HCl was obtained from JT Baker (NJ, USA), and sulfuric acid was obtained from Fisher Chemical (Hampton, NH, USA). Analytical-grade reagents such as hexane, methanol, and MTBE (methyl tertbutyl ether) were purchased for the carotenoid extractions from Extrasynthèse (Genay, France). LC-MS grade solvents were purchased from Sigma-Aldrich (Milan, Italy). Carotenoid standards, namely,  $\beta$ -carotene and lycopene, were purchased from Extrasynthèse (Genay, France).

For the emulsion, refined sunflower oil (Premier, Lloreda S.A., Colombia), drinking water (Crystal, Postobón S.A., Colombia), xanthan gum (MadreTierra, Colombia), and soy lecithin (Ancestral, San Jorge, Colombia) were used. All ingredients used were natural and food-grade.

**Physicochemical Characterization of Peach Palm Fruit Peel.** The chemical composition of different samples was determined following the procedures published by AOAC.<sup>41</sup> Dry matter content was determined gravimetrically by drying each sample at  $105$  °C until a constant weight was reached. The sample water activity (*a<sub>w</sub>*) was measured using a Meter AquaLab 4 TE instrument (Washington, USA). Titratable acidity was determined by volumetry, and the results were expressed as a percentage of citric acid. The pH was determined by using a pHmeter Mettler Toledo S20 SevenEasy (Greifensee, Switzerland). The ash content of the flours was determined gravimetrically at  $550$ – $600$  °C. The lipid content was determined by the Soxhlet method using petroleum ether as a solvent. Protein content was determined by the Kjeldahl method by using a Nitro J.P. Selecta (Barcelona, Spain) equipment, and crude fiber was measured by digestion. Carbohydrate content was determined by the difference. All of the measurements were performed in triplicate.

The color of the samples (flours and emulsions) was measured by tristimulus colorimetry using a Konica Minolta CR-400 colorimeter (Tokyo, Japan) with a D<sub>65</sub> deuterium lamp. The CIELab ( $L^*$ ,  $a^*$ , and  $b^*$ ) coordinates were determined by reflectance. The parameters of chroma ( $C_{ab}^*$ ), hue angle ( $h^\circ$ ), color index ( $IC^*$ ), and total color change ( $\Delta E^*$ ), were calculated using eq 4, as follows:

$$C^* = (a^{*2} + b^{*2})^{1/2} \quad (4)$$

$$h^\circ = \tan^{-1}(b^*/a^*) \quad (5)$$

$$IC^* = (a^* \times 1000)/(L^* \times b^*) \quad (6)$$

$$\Delta E^* = (\Delta a^{*2} + \Delta b^{*2} + \Delta L^{*2})^{1/2} \quad (7)$$

**Carotenoid Analysis.** Carotenoids were analyzed in YVFD, RVFD, YVHAD, and RVHAD samples using the methodology of Stinco et al.<sup>42</sup> For this purpose, 1 g of sample was mixed with 2 mL of *n*-hexane; the mixture was sonicated for 5 min and centrifuged for 10 min at 3000 rpm. The extraction process was repeated three times under the same conditions. The three hexane phases were pooled and concentrated to dryness under a nitrogen stream and stored at  $-20$  °C in the dark until HPLC analyses were performed.

The residue product was reconstituted in 500  $\mu$ L of MeOH/MTBE (1:1, v:v) and then filtered (nylon 0.2  $\mu$ m filter, Pall Life Sciences, Ann Arbor, MI, USA) before being injected into the HPLC. All of the procedures were performed without light. An HPLC instrument was equipped with a photodiode array detector (PDA) SPD-M20A directly connected to the LC column outlet and serially coupled to an LCMS-2020 spectrometer (Shimadzu, Kyoto, Japan) via an atmospheric pressure chemical ionization (APCI) source for mass spectrometry (MS). The chromatographic separation was achieved on a YMC C<sub>30</sub> column (250 mm  $\times$  4.6 mm, 5 mm) column; the mobile phases consisted of methanol/MTBE/water (83:15:2, v/v/v; eluent A) and methanol/MTBE/water (8:90:2, v/v/v; eluent B), using a gradient program as follows: 0 min 0% B; 20 min 20% B; 140 min 100% B. The flow rate was 0.8 mL/min. The injection volume was 20  $\mu$ L. PDA detection was applied in the 200–700 nm range with a sampling frequency of 4.1667 Hz and a time constant of 0.480 s. Chromatograms were extracted at  $\lambda$  450 nm. APCI-MS acquisition was performed in the mass range 100–800 *m/z* with an event time of 0.2 s, scan speed of 5000 u/s, nebulizing gas (N<sub>2</sub>) flow rate of 4 L/min, detector voltage of 0.5 kV, interface temperature of 350 °C, DL (desolvation line) temperature of 300 °C, heat block temperature of 300 °C, and drying gas flow of 5 mL/min. The software LabSolution ver. 5.91 (Shimadzu Corporation) was used for data acquisition.

Carotenoids were identified by their UV-vis and mass spectra, elution order in the C<sub>30</sub> column, and comparison with literature data and the available standard. Quantitative determinations were carried out using the external standard method by previously preparing the calibration curves for  $\beta$ -carotene (1–200  $\mu$ g/mL range,  $r^2 = 0.99$ , LOD = 0.32  $\mu$ g/mL, LOQ = 0.12  $\mu$ g/mL, and CV% = 5) and lycopene (1–100  $\mu$ g/mL range,  $r^2 = 0.99$ , LOD = 0.15  $\mu$ g/mL, LOQ = 0.38  $\mu$ g/mL, CV% = 4). Analyses were performed in triplicate. As reported in the literature,<sup>40</sup> RAE (retinol activity equivalent) was determined only considering  $\beta$ -carotene,  $\alpha$ -carotene, and  $\gamma$ -carotene. NAS-IOM conversion factors, according to RAE =

$\mu\text{g } (\beta\text{-carotene})/12 + \mu\text{g } (\alpha\text{-carotene})/24 + \mu\text{g } (\gamma\text{-carotene})/24$ .

**Phenolic Compound Analysis.** Total phenolic content was determined by the Folin–Ciocalteu spectrophotometric method,<sup>43</sup> using gallic acid as the standard. A solution of the reagent was prepared by a 1:10 dilution of commercial reagent in distilled water; the reagent was protected from light and placed under refrigeration until use. The solutions of each sample were prepared by dilution with ethanol/water (80:20; v/v) and subsequent centrifugation. For each sample, 0.5 mL of sample or standard and 0.5 mL of Folin solution were placed in a flask with 5 mL of water, and after 5 min at 25 °C, the reaction was stopped by adding 1 mL of Na<sub>2</sub>CO<sub>3</sub> 20% solution. Then, the samples were left at 45 °C in a dark place for 15 min. Finally, the absorbance was measured in a spectrophotometer UV–vis Mapada UV 1800 (Shanghai, China) at  $\lambda$  765 nm. The assays were performed in triplicate, and total phenol content was expressed in milligrams of gallic acid equivalent (GAE)/100 g of fruit. The calibration plot showed a 99.6% correlation.

The phenolic compounds were extracted with MeOH/H<sub>2</sub>O (80:20) by a solid–liquid extraction procedure followed by centrifugation.<sup>44</sup> These steps were repeated three times before injection in the HPLC system equipped with a photodiode array detector (PDA) SPD-M20A serially coupled to an LCMS-2020 spectrometer via an electrospray (ESI) source. The separation was achieved on a C<sub>18</sub> Ascentist express column (15 cm × 4.6 mm, 2.7  $\mu\text{m}$ ). The mobile phase was made from solvent A, H<sub>2</sub>O + 0.1 HCOOH, and solvent B, ACN + 0.1 HCOOH, and the gradient was 0–50 min 1–50% B, 50–55 min 50–99% B, 55–60 min 99% B. The flow rate was 1 mL/min, and the injection volume was 5  $\mu\text{L}$ . ESI-MS acquisition was performed in the mass range 100–1000  $m/z$  with an event time of 1 s. Nebulizing and drying gas (N<sub>2</sub>) were set at 1 and 10 L/min, respectively; 1 DL and the heat block temperature were set at 300 and 350 °C, respectively. PDA detection was applied in the 200–700 nm range with a sampling frequency of 4.1667 Hz and a duration of 0.480 s. Chromatograms were extracted at  $\lambda$  280 nm. Identifications were based on UV–vis and mass spectra, as well as relative retention time on a C<sub>18</sub> column, together with published data and a homemade laboratory library. However, the absolute quantitation of the compounds was not performed because of lack of fresh standards at the time of this study; therefore, the corresponding occurrence as relative % was only reported.

**Obtention of Carotenoid-Rich Emulsion-Based Delivery System.** The carotenoid pigments were extracted using sunflower oil as an extraction solvent (green solvent). High shear homogenization was applied according to the method reported by Baria et al.<sup>45</sup> with some modifications. Initially, the peach palm epicarp flour (RVHAD) and sunflower oil mixture were macerated for 15 min (48.8 mL/g liquid–solid ratio) until the colored oil was obtained. Then, the mixture was taken to an Ultraturrax homogenizer (T 25 digital, IKA, Germany) at a stirring speed of 19 200 rpm, for 76 s in a thermal bath at 50 ± 2 °C, with the internal temperature of the sample being less than 30 ± 2 °C. The mixture was centrifuged for 10 min at 14 000g, and the supernatant was subsequently separated to obtain the carotenoid-rich oil extract.

The independent variables, % oil (carotenoid-rich oil extract), % emulsifiers, ultrasonic power (W), and time (min) were defined by previous tests and varied depending on the ranges specified in the CCD design matrix, as shown in Table 2S (Supporting Information). The carotenoid-rich oil

extract (oil phase) and water (aqueous phase) were used as dispersed and continuous phases, respectively. A total weight of 100 g was used as a calculation basis in the preparation of all formulations, with the aqueous phase being the remaining percentage of the sum of the oil phase and the emulsifiers (soy lecithin and xanthan gum in a 1:4 ratio). Initially, the emulsifiers were heated with constant stirring for approximately 1 h at 58 ± 2 °C until completely dissolved in the aqueous phase. Subsequently, the mixture was allowed to cool to 30 ± 2 °C, and the oil phase was slowly added. To form the pre-emulsions, the resulting mixture in each formulation was homogenized in an Ultraturrax disperser (T 25 digital, IKA, Germany) for 3 min at 8000 rpm.<sup>46</sup> In the second stage, the thick emulsions (pre-emulsions) were subjected to ultrasound treatment until the final emulsions (O/W) were obtained. An ultrasonic processor (Ultrasonic Cell Disruptor JY98-IIIDN, China) was equipped with a 15 mm probe, with an ultrasound frequency of 20 kHz and programmed in 5 s on and 5 s off mode. The ultrasonic system was conditioned with an ice bath to maintain the temperature of the samples below 30 ± 2 °C.

**Optimization of Carotenoid-Rich Emulsion-Based Delivery System.** The optimization was conducted to find the ultrasonic conditions and formulation with the highest carotenoid content and the lowest droplet size and polydispersity index. A response surface methodology with a central rotational composite design (CCD) of 29 experiments was applied, where 16 are factorial points, eight are axial points, and five are central points. The coded  $-\alpha$  (−2), −1, 0, +1, + $\alpha$  (+2) and experimental factors used in the study are presented in Table 2S. The experimental variables were X<sub>1</sub>, oil (%); X<sub>2</sub>, emulsifiers (%); X<sub>3</sub>, ultrasonic power (W); and X<sub>4</sub>, time (min). The response variables were represented by three response surface functions: carotenoid content (Y<sub>1</sub>), droplet size (Y<sub>2</sub>), and polydispersity index (Y<sub>3</sub>), each of which was evaluated in triplicate. The derringer desirability function was used to generate optimal conditions for the emulsion formulation. To determine the model validity, the predicted values of the response variables were compared with those obtained under the optimal conditions.

**Emulsion Characterization.** The following physicochemical characteristics were measured on the optimized emulsion during 35 days of storage at 30 ± 2 °C.

**Carotenoid Content.** The quantification of the total carotenoid content ( $\mu\text{g/g}$ ) in the emulsions and flours was determined by spectrophotometry according to the methodology reported by Ordoñez-Santos et al.,<sup>47</sup> using a molar extinction coefficient of  $7.10 \times 10^4 \text{ M}^{-1}\text{cm}^{-1}$  and sunflower oil as a blank, in a Thermo Spectronic Genesys 20 spectrophotometer (USA) at  $\lambda$  464 nm.

**Droplet Size and Polydispersity Index (PDI).** These characteristics were measured using the DLS (dynamic light scattering) technique on a Malvern Zetasizer Nano ZS (United Kingdom). The lipid dispersed phase's refractive index was 1.46. The samples were diluted in deionized water 1:100 (w/w) to avoid multiple dispersion effects.

**Phase Separation.** The phase separation test, also known as gravity cremation, was monitored visually. The samples were stored at 30 ± 2 °C and monitored on days 0, 7, 21, and 35. Additionally, the optimized emulsion was subjected to alternating freezing/thawing cycles (−4 ± 2 °C for 12 h and then at 30 ± 2 °C for 12 h, for 1 week) and thermal stress cycles using an oven (Binder ED 53 UL, GmbH, Germany) with controlled temperature from 40 ± 2 °C to 90 ± 2 °C with

an increment of  $10 \pm 2$  °C every 24 h according to the method proposed by Edris and Malone.<sup>48</sup> The results were reported depending on the case as “stable” (there is no phase separation) and “unstable” (if there is phase separation).

**Conductivity, Turbidity, Viscosity, and Z Potential Measurements.** The conductivity was determined using a portable conductivity meter model 450 (Oakton, Thermo Fisher Scientific) and reported in  $\mu\text{s}/\text{cm}$ . For the determination of turbidity, the samples were diluted in 1:100 (w/w) deionized water, and the measurements were expressed in a nephelometric turbidity unit (NTU) using a portable turbidimeter (AL 250 TR-IR, Maser). Viscosity was measured using a digital viscometer (Model DV-E, Brookfield Engineering Laboratories Inc., MA, USA) at  $30 \pm 2$  °C, with an SC 4–18 spindle at 100 rpm, and reported in centipoise (cP). Zeta potential measurements were performed using a Zeta-Meter System 4.0 (Staunton, USA). The samples were diluted in deionized water 1:100 (w/w) to avoid multiple dispersion effects. They were deposited in capillary cells equipped with two electrodes.

**Morphology.** A confocal laser scanning microscope on a device (Leica Stellaris 5, DMI 8 with LAS 1011, Tokyo, Japan) and transmission electron microscopy (TEM) on a JEOL (JEM-1011, Tokyo, Japan) at 80 kV and 10 k $\times$  magnification were used. The samples were diluted in deionized water (1:10 v/v), and a drop of the dilution was deposited on a copper grid with a Formvar-carbon support and 300 mesh, with uranyl acetate (2% w/v) as a control standard.

**Stability Study.** The stability of the optimized emulsion under stress conditions was investigated by evaluating the percentage of carotenoid retention under different conditions of temperature variation and exposure to light and nitrogen gas according to the methodology reported by Ordóñez-Santos et al.,<sup>49</sup> with some modifications. The percentage of total carotenoid retention was determined according to eq 8:

$$\%R = \frac{C_a}{C_b} \times 100 \quad (8)$$

where  $C_a$  refers to the carotenoid content after treatment and  $C_b$  refers to the carotenoid content in the emulsion before treatment.

The stability to heat treatment was evaluated by subjecting the emulsion to different temperature conditions (25, 30, 40, 50, 50, 70, 80, and 90 °C) for 10 min in a controlled thermal bath (Julabo, Germany) with an uncertainty of  $\pm 2$  °C in all measurements. After each treatment, the samples were cooled in an ice bath until they reached  $10 \pm 2$  °C. For light stability, the emulsion was stored in a refrigerator at  $4 \pm 2$  °C and relative humidity of 85%, adapted with a 25 W lamp located 20 cm above the samples and monitored during 0, 5, 10, 15, 20, 25, 30, and 35 days. In turn, the emulsion was put in contact with nitrogen gas at room temperature at different times (0, 2, 4, 6, 8, and 10 h) using a hermetically sealed capsule coupled to a vacuum pump and saturated with nitrogen gas injection. To evaluate the oxidative stability of the emulsion, the peroxide index was determined under different temperature conditions (25, 30, 40, 50, 60, 70, 80, and 90 °C) for 10 min in a controlled thermal bath (Julabo, Germany) with an uncertainty of  $\pm 2$  °C in all measurements. The determination of the peroxide index was carried out following official method no. 965.33 of the AOAC.<sup>41</sup> For that purpose, 5 g of the emulsion was mixed with 30 mL of a glacial acetic acid and chloroform (3:2) solution and 0.5 mL of a saturated potassium

iodide (KI) solution. After 1 min of controlled stirring in the dark, 30 mL of distilled water was added. It was slowly titrated with a 0.01 N solution of sodium thiosulfate ( $\text{Na}_2\text{S}_2\text{O}_3$ ) using 0.5 mL of a 1% soluble starch solution as an indicator. The peroxide index was calculated using eq 9:

$$\text{PI} \left( \frac{\text{meq O}_2}{\text{kg}} \right) = \frac{(B - S) \times N \times 1000}{W} \quad (9)$$

where  $B$  is the blank titration value,  $S$  is the sample titration value,  $N$  is the normality of sodium thiosulfate, 1000 is the conversion factor (kg), and  $W$  is the sample weight.

**Statistical Analysis.** The Design Expert statistical software (Version 11, Stat-Easy, Godward, MN, USA) was used for experimental design optimization, data analysis, and construction of the second-order polynomial model. The effect of the factors on the variables of interest was identified with an ANOVA test ( $p < 0.05$ ), and the reliability of the model was evaluated with the coefficient of determination  $R^2$ , lack of fit, and coefficient of variation. The emulsion characterization and stability tests were performed by using a randomized, balanced single-factor experiment. An ANOVA analysis and a Tukey test were performed. Statistical analysis was performed using SPSS Windows 18 software.

## ■ ASSOCIATED CONTENT

### Supporting Information

The Supporting Information is available free of charge at <https://pubs.acs.org/doi/10.1021/acsomega.4c03095>.

HPLC–PDA–MS analysis of phenolic compounds in (*Bactris gasipaes*) fruit peels, analysis of variance (ANOVA) of the response surfaces of quadratic equations, and independent variables and code levels of the experimental design (PDF)

## ■ AUTHOR INFORMATION

### Corresponding Author

**Coralía Osorio** – Departamento de Química, Universidad Nacional de Colombia-Sede Bogotá, Bogotá 111321, Colombia; [orcid.org/0000-0001-6222-0138](https://orcid.org/0000-0001-6222-0138); Phone: +57-601-3165000; Email: [cosorio@unal.edu.co](mailto:cosorio@unal.edu.co); Fax: +57-601-3165220

### Authors

**Jader Martínez-Girón** – Facultad de Ingeniería y Administración, Departamento de Ingeniería, Universidad Nacional de Colombia-Sede Palmira, Palmira, Valle del Cauca 763533, Colombia; Tecnología de Procesamiento de Alimentos, Universidad del Valle-Seccional Palmira, Palmira, Valle del Cauca 763531, Colombia

**Cinzia Cafarella** – Messina Institute of Technology c/o Department of Chemical Biological, Pharmaceutical and Environmental Sciences, former Veterinary School, University of Messina, Messina 98122, Italy

**Francesca Rigano** – Messina Institute of Technology c/o Department of Chemical Biological, Pharmaceutical and Environmental Sciences, former Veterinary School, University of Messina, Messina 98122, Italy

**Daniele Giuffrida** – Department of Biomedical, Dental, Morphological and Functional Imaging Sciences, University of Messina, Messina 98122, Italy

**Luigi Mondello** – Messina Institute of Technology c/o Department of Chemical Biological, Pharmaceutical and

Environmental Sciences, former Veterinary School, University of Messina, Messina 98122, Italy; Chromaleont s.r.l., c/o Department of Chemical, Biological, Pharmaceutical and Environmental Sciences, former Veterinary School, University of Messina, Messina 98122, Italy

**Yolima Baena** – *Departamento de Farmacia, Facultad de Ciencias, Universidad Nacional de Colombia-Sede Bogotá, Bogotá 111321, Colombia*

**Luis Eduardo Ordóñez-Santos** – *Facultad de Ingeniería y Administración, Departamento de Ingeniería, Universidad Nacional de Colombia-Sede Palmira, Palmira, Valle del Cauca 763533, Colombia*

Complete contact information is available at:

<https://pubs.acs.org/10.1021/acsomega.4c03095>

## Funding

The authors greatly acknowledge the financial support of Universidad Nacional de Colombia-Sede Palmira (Project No. 57499), Universidad del Valle-Seccional Palmira, and Minciencias-Colombia, C #909. Shimadzu Corporation and Merck Life Science are also acknowledged for their continuous support.

## Notes

The authors declare no competing financial interest.

## ACKNOWLEDGMENTS

The ANLA and Ministry of Environment and Sustainable Development granted permission to collect samples (Framework Agreement for Access to Genetic Resources and their Derivative Products No. 357 of November 17, 2022 signed between the Ministry of Environment and Sustainable Development and the National University of Colombia).

## REFERENCES

- (1) Ding, Z.; Ge, Y.; Sar, T.; Kumar, V.; Harirchi, S.; Binod, P.; Sirohi, R.; Sindhu, R.; Wu, P.; Lin, F.; Zhang, Z.; Taherzadeh, M. J.; Awasthi, M. K. Valorization of tropical fruits waste for production of commercial biorefinery products – A review. *Bioresour. Technol.* **2023**, *374*, No. 128793.
- (2) Sharma, M.; Usmani, Z.; Gupta, V. K.; Bhat, R. Valorization of fruits and vegetable wastes and by-products to produce natural pigments. *Crit. Rev. Biotechnol.* **2021**, *41*, 535–563.
- (3) Can-Cauich, A. C.; Sauri-Duch, E.; Betancur-Ancona, D.; Chel-Guerrero, L.; González-Aguilar, G. A.; Cuevas-Glory, F. L.; Pérez-Pacheco, E.; Moo-Huchin, V. M. Tropical fruit peel powders as functional ingredients: Evaluation of their bioactive compounds and antioxidant activity. *J. Funct. Foods* **2017**, *37*, 501–506.
- (4) Agronet. Ministerio de Agricultura de Colombia: Sistemas de estadísticas agropecuarias. Consulted February 2024. Available online: <http://www.agronet.gov.co>.
- (5) Noronha-Matos, K. A.; Praia Lima, D.; Pereira-Barbosa, A. P.; Zerlotti Mercadante, A.; Campos Chisté, R. Peels of tucumã (*Astrocaryum vulgare*) and peach palm (*Bactris gasipaes*) are by-products classified as very high carotenoid sources. *Food Chem.* **2019**, *272*, 216–221.
- (6) Martínez-Girón, J.; Rodríguez-Rodríguez, X.; Pinzón-Zarate, L. X.; Ordóñez-Santos, L. E. Caracterización fisicoquímica de harina de residuos del fruto de chontaduro (*Bactris gasipaes* Kunth, Arecaceae) obtenida por secado convectivo. *Corpoica Cienc. y Tecnol. Agropecu.* **2017**, *18*, 599–613.
- (7) Martínez-Girón, J.; Ordóñez-Santos, L. E. Determinación de la concentración de pigmentos carotenoides en harina de residuos de chontaduro (*Bactris gasipaes*). *Prod. + Limpia* **2016**, *11*, 85–93.
- (8) Menezes Silva, J. V.; Silva Santos, A.; Araujo Pereira, G.; Campos Chisté, R. Ultrasound-assisted extraction using ethanol efficiently

extracted carotenoids from peels of peach palm fruits (*Bactris gasipaes* Kunth) without altering qualitative carotenoid profile. *Heliyon* **2023**, *9*, No. e14933.

(9) Santos, Y. J. S.; Facchinatto, W. M.; Rochetti, A. L.; Carvalho, R. A.; Le Feunteun, S.; Fukumasu, H.; Morzel, M.; Colnago, L. A.; Vanin, F. J. Systemic characterization of pupunha (*Bactris gasipaes*) flour with views of polyphenol content on cytotoxicity and protein *in vitro* digestion. *Food Chem.* **2023**, *405*, 134888.

(10) Chisté, R. C.; Costa, E. L. N.; Monteiro, S. F.; Mercadante, A. Z. Carotenoid and phenolic compound profiles of cooked pulps of orange and yellow peach palm fruits (*Bactris gasipaes*) from the Brazilian Amazonia. *J. Food Comp. Anal.* **2021**, *99*, 103873.

(11) Saini, R. K.; Nile, S. H.; Park, S. Carotenoids from fruits and vegetables: Chemistry, analysis, occurrence, bioavailability and biological activities. *Food Res. Int.* **2015**, *76*, 735–750.

(12) Rodríguez-Concepción, M.; Avalos, J.; Bonet, M. L.; Boronati, A.; Gómez-Gómez, L.; Hornero-Méndez, D.; Limon, M. C.; Meléndez-Martínez, A. J.; Olmedilla-Alonso, B.; Palou, A.; Ribot, J.; Rodrigo, M. J.; Zacarias, L.; Zhu, Ch. A global perspective on carotenoids: Metabolism, biotechnology, and benefits for nutrition and health. *Prog. Lipid Res.* **2018**, *70*, 62–93.

(13) Boonlao, N.; Ruktanonchai, U. R.; Anal, A. K. Enhancing bioaccessibility and bioavailability of carotenoids using emulsion-based delivery systems. *Colloids Surf.: Biointerfaces* **2022**, *209*, 112211.

(14) Gomes, A.; Costa, A. L. R.; Sobral, P. J. d. A.; Cunha, R. L. Delivering  $\beta$ -carotene from O/W emulsion-based systems: Influence of phase ratio and carrier lipid composition. *Food Hydrocoll. Health* **2023**, *3*, 100125.

(15) de Souza Mesquita, L. M.; Neves, B. V.; Pisani, L. P.; de Rosso, V. V. Mayonnaise as a model food for improving the bioaccessibility of carotenoids from *Bactris gasipaes* fruits. *LWT–Food Sci. Technol.* **2020**, *122*, 109022.

(16) Vo, T. P.; Tran, H. K. L.; Ta, T. M. N.; Nguyen, H. T. V.; Phan, T. H.; Nguyen, T. H. P.; Nguyen, V. K.; Dang, T. C. T.; Nguyen, L. G. K.; Chung, T. Q.; Nguyen, D. Q. Extraction and emulsification of carotenoids from Carrot pomaces using oleic acid. *ACS Omega* **2023**, *8*, 39523–39534.

(17) Taha, A.; Ahmed, E.; Ismaiel, A.; Ashokkumar, M.; Xu, X.; Pan, S.; Hu, H. Ultrasonic emulsification: An overview on the preparation of different emulsifiers-stabilized emulsions. *Trends Food Sci. Technol.* **2020**, *105*, 363–377.

(18) Zhou, L.; Zhang, J.; Xing, L.; Zhang, W. Applications and effects of ultrasound assisted emulsification in the production of food emulsions: A review. *Trends Food Sci. Technol.* **2021**, *110*, 493–512.

(19) Niu, B.; Shao, P.; Sun, P. Ultrasound-assisted emulsion electrospayed particles for the stabilization of  $\beta$ -carotene and its nutritional supplement potential. *Food Hydrocoll* **2020**, *102*, 105634.

(20) Jin, Y.; Tang, J.; Sablani, S. S. Food component influence on water activity of low-moisture powders at elevated temperatures in connection with pathogen control. *LWT–Food Sci. Technol.* **2019**, *112*, 108257.

(21) Teixeira, G. L.; Ibañez, E.; Block, J. M. Emerging lipids from Arecaceae palm fruits in Brazil. *Molecules* **2022**, *27*, 4188.

(22) Morais, R. A.; Teixeira, G. L.; Ferreira, S. R. S.; Cifuentes, A.; Block, J. M. Nutritional composition and bioactive compounds of native Brazilian fruits of the Arecaceae family and its potential applications for health promotion. *Nutrients* **2022**, *14*, 4009.

(23) Hassan, A. F.; Ismail, A.; Hamid, A. A.; Azlan, A.; Al-sheraji, S. H. Characterisation of fibre-rich powder and antioxidant capacity of Mangifera pajang K. fruit peels. *Food Chem.* **2011**, *126*, 283–288.

(24) Nagarajaiah, S. B.; Prakash, J. Chemical composition and antioxidant potential of peels from three varieties of banana. *As. J. Food Ag-Ind.* **2011**, *4*, 31–46.

(25) Rojas-Garbanzo, C.; Pérez, A. M.; Bustos-Carmona, J.; Vaillant, F. Identification and quantification of carotenoids by HPLC-DAD during the process of peach palm (*Bactris gasipaes* H.B.K.) flour. *Food Res. Int.* **2011**, *44*, 2377–2384.

(26) González-Peña, M. A.; Ortega-Regules, A. E.; Anaya de Parrodi, C.; Lozada-Ramírez, J. D. Chemistry, occurrence, properties,

- applications, and encapsulation of carotenoids-A review. *Plants* **2023**, *12*, 313.
- (27) Britton, G.; Khachik, F. *Carotenoids in Food*; Britton, G., Liaaen-Jensen, S., Pfander, H., Verlag, B., Eds.; Carotenoids: Basel, 2009.
- (28) Rade, D.; Mokrovčak, Ž.; Strucelj, D.; Skevin, D.; Nederal, S. The Effect of processing conditions on the nontriacylglycerol constituents of sunflower oil. *Acta Aliment* **2004**, *33*, 7–18.
- (29) Ordóñez-Santos, L. E.; Pinzón-Zarate, L. X.; González-Salcedo, L. O. Optimization of ultrasonic-assisted extraction of total carotenoids from peach palm fruit (*Bactris gasipaes*) by-products with sunflower oil using response surface methodology. *Ultrason. Sonochem.* **2015**, *27*, 560–566.
- (30) Vo, T. P.; Tran, H. K. L.; Ta, T. M. N.; Nguyen, H. T. V.; Phan, T. H.; Nguyen, T. H.P.; Nguyen, V. K.; Dang, T. C. T.; Nguyen, L. G. K.; Chung, T. Q.; Nguyen, D. K. Extraction and emulsification of carotenoids from carrot pomaces using oleic acid. *ACS Omega* **2023**, *8*, 39523–39534.
- (31) Leong, T. S. H.; Manickam, S.; Martin, G. J.; Li, W.; Ashokkumar, M. *Ultrasonic Production of Nano-emulsions for Bioactive Delivery in Drug and Food Applications*; Springer: Berlin, Germany, 2018; Vol. 46.
- (32) Alzorqi, I.; Ketabchi, M. R.; Sudheer, S.; Manickam, S. Optimization of ultrasound induced emulsification on the formulation of palm-olein based nanoemulsions for the incorporation of antioxidant  $\beta$ -D-glucan polysaccharides. *Ultrason. Sonochem.* **2016**, *31*, 71–84.
- (33) Borba, C. M.; Tavares, M. N.; Macedo, L. P.; Araújo, G. S.; Furlong, E. B.; Dora, C. L.; Burkert, J. F.M. Physical and chemical stability of  $\beta$ -carotene nanoemulsions during storage and thermal process. *Food Res. Int.* **2019**, *121*, 229–237.
- (34) Mozafarpour, R.; Koocheki, A. Fabrication of emulsion gels based on sonicated grass pea (*Lathyrus sativus* L.) protein as a delivery system for  $\beta$ -carotene: Kinetic modeling and release behaviour. *LWT - Food Sci. Technol.* **2023**, *184*, 115020.
- (35) McClements, D. J. Edible nanoemulsions: fabrication, properties, and functional performance. *Soft Matter* **2011**, *7*, 2297–2316.
- (36) Singh, P.; Kaur, G.; Singh, A. Physical, morphological and storage stability of clove oil nanoemulsion based delivery system. *Food Sci. Technol. Int.* **2023**, *29*, 156–167.
- (37) Meléndez-Martínez, A. J.; Esquivel, P.; Rodríguez-Amaya, D. B. Comprehensive review on carotenoid composition: Transformations during processing and storage of foods. *Food Res. Int.* **2023**, *169*, 112773.
- (38) López-Monterrubio, D. I.; Lobato-Calleros, C.; Vernon-Carter, E. J.; Alvarez-Ramirez, J. Influence of  $\beta$ -carotene concentration on the physicochemical properties, degradation and antioxidant activity of nanoemulsions stabilized by whey protein hydrolyzate-pectin soluble complexes. *LWT - Food Sci. Technol.* **2021**, *143*, 111148.
- (39) Teixé-Roig, J.; Oms-Oliu, G.; Odriozola-Serrano, I.; Martín-Belloso, O. Emulsion-based delivery systems to enhance the functionality of bioactive compounds: towards the use of ingredients from natural, sustainable sources. *Foods* **2023**, *12*, 1502.
- (40) Gasa-Falcon, A.; Odriozola-Serrano, I.; Oms-Oliu, G.; Martín-Belloso, O. Impact of emulsifier nature and concentration on the stability of  $\beta$ -carotene enriched nanoemulsions during: In vitro digestion. *Food Funct* **2019**, *10*, 713–722.
- (41) AOAC. *Official Methods of Analysis of AOAC International*, 18th ed.; Association of Official Analytical Chemists: Gaithersburg, MD, 2006.
- (42) Stinco, C. M.; Fernández-Vázquez, R.; Escudero-Gilete, M. L.; Heredia, F. J.; Meléndez-Martínez, A. J.; Vicario, I. M. Effect of Orange juicés processing on the color, particle size, and bioaccessibility of carotenoids. *J. Agric. Food Chem.* **2012**, *60*, 1447–1455.
- (43) Singleton, V. L.; Orthofer, R.; Lamuela-Raventós, R. M. Analysis of total phenol and other oxidation substrates and antioxidants by means of Folin–Ciocalteu reagent. *Methods Enzymol.* **1999**, *299*, 152–178.
- (44) Montedoro, G.; Servili, M.; Baldioli, M.; Miniati, E. Simple and hydrolyzable phenolic compounds in virgin olive oil. 1. Their extraction, separation, and quantitative and semiquantitative evaluation by HPLC. *J. Agric. Food Chem.* **1992**, *40*, 1571–1576.
- (45) Baria, B.; Upadhyay, N.; Singh, A. K.; Malhotra, R. K. Optimization of 'green' extraction of carotenoids from mango pulp using split plot design and its characterization. *LWT - Food Sci. Technol.* **2019**, *104*, 186–194.
- (46) Traynor, M.; Burke, R. M.; Frías, J.; Gaston, E.; Barry-Ryan, C. Formation and stability of an oil in water emulsion containing lecithin, xanthan gum and sunflower oil. *Int. Food Res. J.* **2013**, *20*, 2173–2181.
- (47) Ordoñez-Santos, L. E.; Pinzón-Zarate, L. M.; González-Salcedo, L. O. Optimization of ultrasonic of total carotenoids from peach palm fruit (*Bactris gasipaes*) by-products with sunflower assisted extraction oil using response surface methodology. *Ultrason. Sonochem.* **2015**, *27*, 560–566.
- (48) Edris, A. E.; Malone, C. F. R. Preferential solubilization behaviours and stability of some phenolic-bearing essential oils formulated in different microemulsion systems. *Int. J. Cosmet. Sci.* **2012**, *34*, 441–450.
- (49) Ordoñez-Santos, L. E.; Martínez-Girón, J.; Villamizar-Vargas, R. H. Encapsulation of  $\beta$ -carotene extracted from peach palm residues: a stability study using two spray-dried processes. *DYNA* **2018**, *85*, 128–134.